frontiers | Frontiers in Marine Science

TYPE Original Research
PUBLISHED 21 September 2022
DOI 10.3389/fmars.2022.973364

Check for updates

OPEN ACCESS

EDITED BY
Sascha Floegel,
GEOMAR Helmholtz Center for Ocean Research Kiel, (HZ), Germany

REVIEWED BY
Carlo Cerrano,
Marche Polytechnic University, Italy
Fernando Tuya,
University of Las Palmas de Gran Canaria, Spain

*CORRESPONDENCE
Andreia Braga-Henriques
braga.henriques02@gmail.com

SPECIALTY SECTION
This article was submitted to Deep-Sea Environments and Ecology, a section of the journal Frontiers in Marine Science

RECEIVED 20 June 2022
ACCEPTED 12 August 2022
PUBLISHED 21 September 2022

CITATION
Braga-Henriques A, Buhl-Mortensen P, Tokat E, Martins A, Silva T, Jakobsen J, Canning-Clode J, Jakobsen K, Delgado J, Voirand T and Biscoito M (2022) Benthic community zonation from mesophotic to deep sea: Description of first deep-water kelp forest and coral gardens in the Madeira archipelago (central NE Atlantic). *Front. Mar. Sci.* 9:973364. doi: 10.3389/fmars.2022.973364

COPYRIGHT
© 2022 Braga-Henriques, Buhl-Mortensen, Tokat, Martins, Silva, Jakobsen, Canning-Clode, Jakobsen, Delgado, Voirand and Biscoito. This is an open-access article distributed under the terms of the Creative Commons Attribution License (CC BY). The use, distribution or reproduction in other forums is permitted, provided the original author(s) and the copyright owner(s) are credited and that the original publication in this journal is cited, in accordance with accepted academic practice. No use, distribution or reproduction is permitted which does not comply with these terms.

Benthic community zonation from mesophotic to deep sea: Description of first deep-water kelp forest and coral gardens in the Madeira archipelago (central NE Atlantic)

Andreia Braga-Henriques[1,2,3,4]*, Pål Buhl-Mortensen[5], Erdal Tokat[6], Ana Martins[6,7], Teresa Silva[2,8], Joachim Jakobsen[9], João Canning-Clode[1,2,10], Kirsten Jakobsen[9], João Delgado[2,11], Thibaut Voirand[12] and Manuel Biscoito[1,2,3]

[1]MARE – Marine and Environmental Sciences Centre, ARNET - Aquatic Research Network, Agência Regional para o Desenvolvimento da Investigação Tecnologia e Inovação (ARDITI), Funchal, Portugal, [2]OOM – Oceanic Observatory of Madeira, Funchal, Portugal, [3]Museu de História Natural do Funchal, Estação de Biologia Marinha do Funchal, Funchal, Portugal, [4]Regional Directorate for Fisheries, Regional Secretariat for the Sea and Fisheries, Government of the Azores, Horta, Portugal, [5]Benthic Communities and Coastal Interactions Research Group, Institute of Marine Research (IMR), Bergen, Norway, [6]OKEANOS — Institute of Research in Marine Sciences, Horta, Portugal, [7]DOP – Department of Oceanography and Fisheries, Faculty of Sciences and Technology, University of the Azores, Horta, Portugal, [8]MARE – Marine and Environmental Sciences Centre, ARNET - Aquatic Research Network, Faculty of Sciences of the University of Lisbon, Lisboa, Portugal, [9]Rebikoff-Niggeler Foundation, Horta, Portugal, [10]Smithsonian Environmental Research Center, Edgewater, MD, United States, [11]Regional Directorate for Sea, Direção de Serviços de Monitorização, Estudos e Investigação do Mar (DSEIMar), Regional Government of Madeira, Funchal, Portugal, [12]Telespazio France, GeoInformation Business Unit, Latresne, France

The Madeira archipelago has a unique underwater landscape that is characterised by narrow shelves, steep slopes and a large submarine tributary system that boosts primary productivity in oligotrophic waters and thus offers a potential for hotspots of biodiversity. Despite this, there have been limited deep-water exploration activities with less than five expeditions since the 1960s. Here, we investigated the seabed on the southern side of the Madeira-Desertas Ridge using a manned submersible along a 3.8 km long transect starting at 366 m depth up the ridge shelf until its top at 73 m. Benthic habitats and community composition were documented with video along a depth gradient from mesophotic to deep sea. Six distinct biotopes were recognised (three deeper, and three shallower than 115 m depth). Our results showed a rich biodiversity with deep biotopes characterised by sponges and non-reef-building corals (e.g., *Pachastrella monilifera*, *Viminella flagellum*, *Eunicella verrucosa*) and shallow biotopes comprising macroalgae and the gorgonian *Paramuricea* cf. *grayi*. The pronounced benthic zonation reflects the

Abbreviations: MADM, Herbarium of the Funchal Natural History Museum.

steep environmental gradient that includes high topographic variation, heterogeneous substrates, and bidirectional regular wave-motion at the shallow mesophotic part. Together with biotic factors, such as low density of sea urchins and presence of predatory fish, this environment with unusual deep light penetration, a mesoscale cyclonic eddy, and deep wave-motion, has allowed the establishment of a mature deep-water kelp population of *Laminaria ochroleuca* in the plateau (max. >100 individuals p/100 m^2). At the same time, a conspicuous coral fauna was observed on a wide range of soft to hard bottoms with several species taking advantage of the favourable hydrodynamic regime and seawater properties together with substratum availability to create coral gardens. These habitats were previously not known from Madeira, and their newfound discovery in the archipelago merit further investigation and protection.

KEYWORDS

Vulnerable Marine Ecosystems (VMEs), macroalgae, megabenthic communities, Macaronesia, image analysis, environmental drivers, Octocorallia, Marine Animal Forests (MFAs)

Introduction

To protect and sustainably manage marine benthic ecosystems from human activities and environmental changes, it is crucial to know what species and habitats occur there, how these are structured and what factors may shape their distribution (e.g., Convention on Biological Diversity Aichi Biodiversity Target 11 or UN Sustainable Development Goal 14). As such, underwater exploration to provide biodiversity data from uncharted areas has steadily increased, which has contributed to the accelerated discovery of deep-water conspicuous marine realms, including at mesophotic depths. These ecosystems are characterised by the presence of light-dependent communities around ~30–150 m depth, and have been documented from both oceanic, insular and continental slope areas (Loya et al., 2019). Our understanding of these ecosystems is mostly supported by descriptions from underwater surveys in tropical and subtropical ecoregions on what is known as mesophotic coral ecosystems – MCEs (Lesser et al., 2009), but increased research efforts stretch them to temperate regions, particularly coralligenous areas of the Mediterranean Sea (Bo et al., 2011; Ponti et al., 2018) and more recently of the West Iberian margin (Boavida et al., 2016).

Species richness and assemblage composition may vary according to environmental settings (Borcard et al., 1992), but the main components of temperate mesophotic ecosystems (TMEs) comprise of macroalgae that are commonly associated with megabenthic suspension feeders, such as corals and sponges (Cerrano et al., 2019 and references therein). Irradiance of photosynthetically active radiation (PAR, 400–700 nm) is the most significant abiotic factor controlling the bathymetric distribution of mesophotic ecosystems. The depth at which PAR is about 1% of surface irradiance is commonly used to define the lower limit of the euphotic zone (Clarke, 1936; Ryther, 1956). However, photoautotrophic organisms may still occur below this PAR's percentage (Lesser et al., 2009).

The Madeira archipelago has a unique underwater landscape characterised by shelf breaks very close to the shoreline, steep slopes and large submarine tributary systems (Quartau et al., 2018). Current-topography interactions on these features underlying oligotrophic surface waters (Longhurst, 1995) induce local upwelling and enhance biological productivity at the euphotic zone, thus offering a potential for hotspots of biodiversity (Gove et al., 2016). Despite this, there have been few deep-water exploration activities in Madeira, with less than five expeditions since the 1960s that resulted only in a handful of video transects (Bathyscaphe *Archimède* in 1966; HOV *Johnson-Sea-Link I* in 1991; ROV *Luso* in 2010 and 2018). The few reports available have identified the presence of a number of sponges and corals with erect growth forms (CNEXO, 1972; Reed and Pomponi, 1992) that under favourable conditions can create dense and three-dimensional assemblages, which in part are structurally and functionally similar to terrestrial forests known as 'Marine Animal Forests' – MAFs (Rossi et al., 2017). These habitats sustain high biodiversity, including fish (adults and juveniles), have a key role in ecosystem functioning (Cerrano et al., 2010; Ponti et al., 2018), and in deep sea represent vulnerable marine ecosystems (VMEs). VMEs share certain attributes (e.g., uniqueness or rarity, functional significance, fragility, and structural complexity) used for assessing their vulnerability to

anthropogenic disturbance that can compromise the integrity of seabed including biodiversity (FAO, 2009; ICES, 2020).

Adding to that, and in line with historical, though non-peer reviewed records (Silva and Menezes, 1940), a large brown algae (kelp of the order Laminariales) was collected beyond the range of recreational scuba diving during the scientific expedition "Monaco Explorations 2017-2020" at the Madeira-Desertas Ridge (A. Braga-Henriques, pers. obs.). Kelp plants are long-lived and create three-dimensional biological habitats (Graham et al., 2007). They grow in dense stands with pronounced primary production rates (up to ≥3000 gC m^{-2} $year^{-1}$, Chung et al., 2011), support high levels of biodiversity (Teagle et al., 2018), and have an important role in the organic matter cycling (Pessarrodona et al., 2018). The ecological services they provide represent great economic value (Beaumont et al., 2008), but are likely to degrade rapidly over the next decades due to climate and human-induced changes in the marine environment that have led so far to biomass losses of about 2% per year (Wernberg et al., 2019). Deep-water kelp forests may offer a buffer against those stressors (e.g., extreme storms, heat waves, overfishing) acting as a refugia, i.e., providing a suitable area for kelp development below inhospitable surface waters (Graham et al., 2007). Despite this, little attention is given to deep kelps partly due to the low number of taxa described from deeper waters and the difficulty to visit these communities.

Together, preliminary discoveries presented herein have underpinned the occurrence of TMEs with potentially unique conservation value in Madeira. Here, we combined visual seabed observations, remote sensing and *in situ* oceanographic data to characterise benthic habitats and biotopes of the Madeira-Desertas Ridge from mesophotic to deep sea. We aim to gather ecological information about assemblage composition, abundances and range shifts across environmental gradients, which are instrumental as input to species distribution models (SDMs) and climatic refugia scenarios. A georeferenced database is created to inform managers, stakeholders and decision makers about the location of the different habitats of conservation interest, identifying direct human-induced disturbances, to facilitate the protection and sustainable management of these biodiversity hotspots.

Material and methods

Study area

Madeira archipelago is located in the subtropical Northeast Atlantic (within the 32.00°–33.00°N and 17.50°–16.00°W belt), at approximately 1000 km southwest of the Iberian margin (Figure 1A). It is of volcanic origin and comprises the main island of Madeira (737Km^2), Porto Santo (42Km^2), Desertas (13Km^2 spanning three narrow islands: Ilhéu Chã, Deserta Grande and Bugio) and Selvagens (~3Km^2). The first three islands represent the youngest geologically section of the Madeira Hotspot track, a chain of volcanic seamounts and islands of >70 Myr old (Geldmacher et al., 2006). The investigated area is located on the Madeira-Desertas Ridge, between the eastern end of Madeira and the Desertas Islands (Figure 1B). It is known for provision of current-swept hard substrate, and a hydrodynamic regime often controlled by the

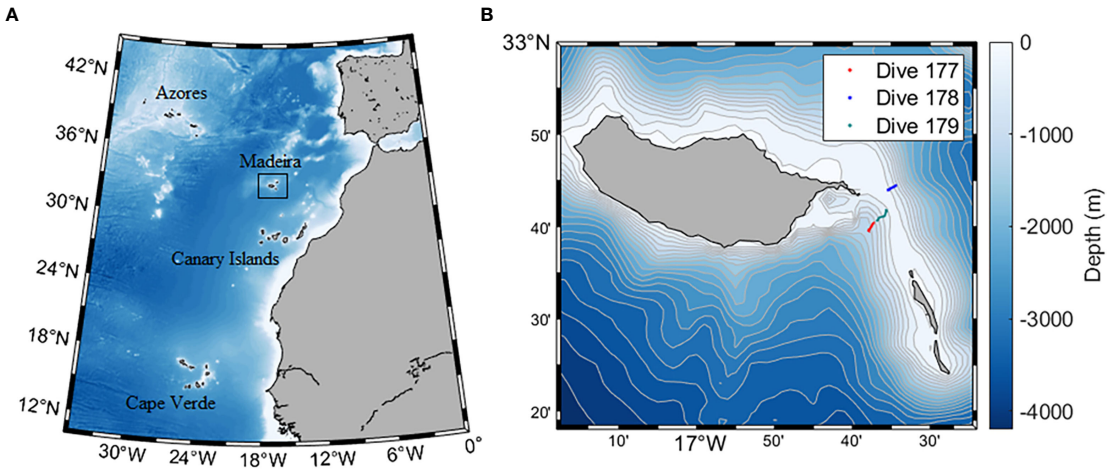

FIGURE 1
(A) Location of Madeira archipelago in the Macaronesia context. **(B)** Detailed map of the location of the surveyed area on the Madeira-Desertas Ridge: Western flank – CTD measurements and seawater collection down to 990 m depth (#177); Eastern flank – CTD measurements and seawater collection down to 926 m depth (#178); and upper Western flank towards the summit crest – CTD measurements, seawater collection and continuous seafloor observations down to 366 m depth (#179).

topography (Campuzano et al., 2010). The Desertas Islands are the expression of a 60 km long submarine ridge, with a submerged part approximately 40 km long and 20 km wide at its basis (Klügel et al., 2005). It rises steeply from around 2500 m depth up to the crest at depths mainly between 100 and 250 m. The deepest point of the ridge crest (ca. 250 m) is located approximately at the middle of the ridge.

The temperature regime is mild and conservative at the Madeira archipelago with seawater surface temperatures around 20.4°C and little seasonal related variation (Schäfer et al., 2019). The lower part of the euphotic zone is located between 90 and 130 m depth (Teira et al., 2005). The region is influenced by the Canary Current (CC), a branch of the North Atlantic Drift, at the boundary of the North Atlantic Subtropical Gyre (NASG), which comprises a relatively shallow flow (i.e., down to about 200-300 m, max. 500 m depth) that brings oligotrophic North Atlantic Central Waters (NACW) from the east (Pelegrí and Peña-Izquierdo, 2015). The CC is wide (about 1000 km) and slow (10-30 $cm.s^{-1}$), flowing year-round towards the Equator (Batten et al., 2000). Its surface waters are relatively cool, ranging from 15 to 20°C, due to the entrainment of upwelled water from the northwest coastal African upwelling system as the CC flows southwards (Mittelstaedt, 1991). The other two large-scale surface current systems are the Azores Current/Front system (AzC/AzF) and the Portugal Current (PC). Located south of the Azores archipelago, the AzC/AzF is part of the NAG and originates as a branch of the warm and saline western boundary current known as the Gulf Stream (GS), near the Grand Banks (40°N, 45°W) (Le Traon and De Mey, 1994). The warm AzC current travels eastwards between 32 and 35° N until it reaches the African coast. Its main current jet is ~150 km wide and 1000 m deep, with average current speeds reaching more than 10 $cm.s^{-1}$. The area near the AzC experiences high eddy kinetic energy. Along its eastward-flowing component, the AzC produces three major southward-flowing branches (Klein and Siedler, 1989). The easternmost branch turns southwards passing south of Madeira and feeding the CC (New et al., 2001). The PC is a weak, warm, broad and slow surface water current resulting from the movement of water east caused by the North Atlantic Drift (NADC) (Otto and van Aken, 1996). The PC generally flows southwards and extends from about 10°W to 24°W, affecting Madeira ocean circulation and dynamics as well.

Submersible surveys

Survey data was collected with the aid of the manned submersible LULA1000 during three dives carried out at the Madeira-Desertas Ridge (Figure 1B): #177 Western flank (WF), 15-10-2019 (start 16° 37.908' W, 32° 39.649' N; end 16° 37.260' W, 32° 40.399' N) – CTD measurements and seawater collection down to 990 m depth; #178 Eastern flank (EF), 16-10-2019 (start 16° 34.422' W, 32° 44.496' N; end 16° 35.448' W, 32° 43.994' N) – CTD measurements and seawater collection down to 926 m; and #179 upper Western flank towards the summit crest (WFS), 18-10-2019 (start 16° 36.794' W, 32° 40.685' N; end 16° 35.634' W, 32° 41.791' N) – CTD measurements, seawater collection and continuous seafloor observations down to 366 m. Sea operations had the support of the vessel *ADA REBIKOFF* for transit to the survey area, underwater positioning and communications to the surface. The sub was equipped with a range of instruments: two ultra HD video cameras (Sony Alpha A III R and Sony PXW-X70, recording device - Atomos Shogun, recording format Apple ProRes 422); 360° sonar; fluxgate compass; DVL; depth sounder; USBL tracking system; a CTD (CTD 60M Sea & Sun Technology GmbH) and associated unit sensors – Vbatt (Volt), Pressure (dbar), Temperature (°C), Conductivity (mS/cm), OxyGd (% and dissolved), Turbidity (FTU); and a hydraulic manipulator arm plus a basket beneath the observation dome providing temporary storage of samples. Geographical positions, time and depth were recorded as navigation files on board the support vessel.

Environmental data (*in situ* and satellite derived)

The oceanographic parameters collected on board LULA1000 were analysed with the incorporated standard data acquisition software and further processed with Surfer (version 10.7) and Grapher (version 8.8) for data visualisation. After removing spikes from the dataset, values were averaged at every one-meter depth interval. Downcast [descent], along bottom, and upcast [ascent] CTD data for each dive were combined to provide an overview of the physical oceanographic context for the study area while downcast profiles down to 150 m depth were plotted to detect transitional water layers. Seawater samples for dissolved inorganic nutrient (nitrate, nitrite, phosphate, and silicate) measurements were also collected along the dive track at the maximum (circa) depth surveyed, potential deep chlorophyll-α maximum – DCM (ca. 80 m), and near the surface. The samples refrigerated on board were further frozen (−20°C) until analysis. Nutrient concentrations were determined by manual methods (Grasshoff et al., 1999) with spectral absorbance measured in a UV-vis spectrophotometer (Shimadzu UVmini-1240).

To infer mesoscale spatial gradients of other parameters that could also best explain species horizontal and vertical distribution (Loya et al., 2019; Jayathilake and Costello, 2020), physical, wave and biogeochemical products from the Copernicus Marine Environment Monitoring Service (CMEMS) were obtained for the time window (October 2019) of the submersible surveys (Supplementary Table S1). Satellite data can detect general patterns of ecological importance and have been used as a reference for real environmental conditions due to its regular and spatially uniform basis (Smale and Wernberg, 2009; Lesser et al., 2019; Tuya et al., 2021). All data

were further processed using the NASA/OB.DAAC data analysis software SeaDASv7.5.3 (https://seadas.gsfc.nasa.gov).

Seabed observations and sampling

Total duration of seabed video recording was three hours and 57 minutes, starting on the south-west side of the ridge and ending at the crest of the ridge at 73 m depth (WFS, dive #179). This transect provided visual documentation of the seabed over a long distance (3 872 m and an area of approximately 15 500 m^2) at an average speed of ~0.3 $m.s^{-1}$. Annotations of general benthic observations and species of particular interest were performed in real time by the scientific observer on board. Samples from representative taxa were collected and kelp plants were stored for genetic analysis to confirm its taxonomic identification (see Supplementary S3 for methodology used).

Video annotation and data treatment

Video footage was reviewed and annotated with the aid of the software VideoNavigator vs 2.1.28.0 (Institute of Marine Research, Norway). Observations of epibenthic organisms >5 cm, lost fishing gear (nylon lines and ropes) and damaged large sessile megafauna were georeferenced based on synchronised video playback and underwater navigational data, hereafter designated as events. These events were recorded along with associated information about time, depth and geographic position. Since many taxa are impossible to identify from imagery and there is limited taxonomic knowledge of deep and mesophotic species for the area, we used operational taxonomic units (OTUs), or morphospecies, to differentiate taxa that could not be identified to a low taxonomic level from the video (Howell et al., 2019). In cases where several individuals occurred within the same video frame, the video was paused, and these were counted. The events were aggregated into subsamples of 50 m sequences along the seabed (hereafter referred to as video samples). The area of the video samples was calculated assuming an average visual field width of 4 m. Overall, our raw dataset comprises 78 video samples that was further used for abundance estimates (number of individuals or colonies per 100 m^2) and multivariate analyses.

Composition of substrate types were estimated as percentage surface coverage along the seabed using six different substrate categories, reflecting the detectable grain-sizes from the video: (1) mud/sandy mud, (2) sand, (3) pebble, (4) cobble, (5) outcropping bedrock, and (6) bedrock with a thin layer of sandy mud. These size classes are based on a modification of the definitions provided by the Wentworth scale (Wentworth, 1922). In addition, the percentage cover of crustose coralline algae was estimated. The coverage was assessed regularly at 30 sec intervals within habitats of homogeneous substrate composition, and more frequently within habitats with more variation in the substrate composition.

Size of kelp plants was estimated using a scale positioned in the sub and they were categorised according to stipe length (cm): small (ca. <30) and large (ca. ≥30). Wave action was assessed inside stands of large individuals based on the movement of the kelp's lamina at places where the position of the sub was optimal for measurements (n = 11 locations). The frequency of the waves was measured as the time from start of motion from one side to stop of motion at the other side. The compass direction of the lamina was estimated at start and stop of this motion. Wave direction was assessed based on the heading of the submersible. The wave lengths were estimated as the distance that the tip of the lamina had moved during the wave motion.

Ordination analyses

The structure of benthic habitats and occurrence of biotopes with characteristic taxa and environmental settings was investigated using two ordination methods with the software PC-Ord (McCune and Mefford, 2006). Prior to the analysis, taxa with uncertain identifications or a broad taxonomic resolution (e.g., "sponge" or "fish") were discarded from the dataset because these would not add relevant information to distinguish classes of video samples. Furthermore, only those video samples with at least four taxa were used. The resulting dataset after the quality treatment consisted of 74 video samples and 49 taxa. Abundance data were square root transformed to down-weight superabundant taxa.

First, we applied an algorithm performing divisive hierarchical ordination (including taxa represented as OTUs) to classify video samples and species using TWINSPAN (two-way indicator species analysis) (Hill, 1979). The data is ordered by the first axis of a correspondence analysis and then split near the middle, adjusted by the identification of indicator species with preferential affiliation to one of the two groups. Each of these groups is then iteratively split again using the same process, producing a hierarchical classification of samples with indicator species for each group. The transformed abundances were allocated to five abundance levels ("pseudo-species" within the TWINSPAN terminology) using the following cut levels: >0–2, 2–5, 5–10, 10–20, and >20. All species meeting these criteria were included in the analysis. Rare species were down-weighted using the corresponding function in PC-Ord.

To identify latent factors that drive observed variation in the abundance of species between the video samples, we then applied a detrended correspondence analysis (DCA) (Hill and Gauch, 1980). The DCA algorithm constructs an iterative reciprocal averaging (Hill, 1973), starting with arbitrary initial sample scores, where weights are the species score data. It is an indirect gradient analysis, where environmental data are "overlaid" onto the ordination plot. The environmental variables (values calculated for each video sample) used in the analysis were: percentage cover of six substrate categories, depth (in m, mean and range), temperature (°C), salinity (PSU), oxygen saturation (%), and turbidity (FTU). Generic bottom types based on the Folk scale and identified TWINSPAN classes were used as categorical variables.

Results

General habitat description

Physical-chemical properties of the water column

The upper water layer was well mixed down to ~75–80 m depths with all [downcast] profiles showing similar surface temperatures (~22.65–22.92°C) and salinities (36.8< S <36.88) (Figures 2, 3). At the WFS (#179), we identified a peak of dissolved oxygen at 35 m depth (3.45 mL.L^{-1}) and a minimum oxygen layer below the mixed layer depth (MLD) (1.32 mL.L^{-1} at 105 m depth). Underneath the MLD, a seasonal thermocline and halocline are clearly detected in all stations. Water characteristics indicate the presence of the East North Atlantic Central Water

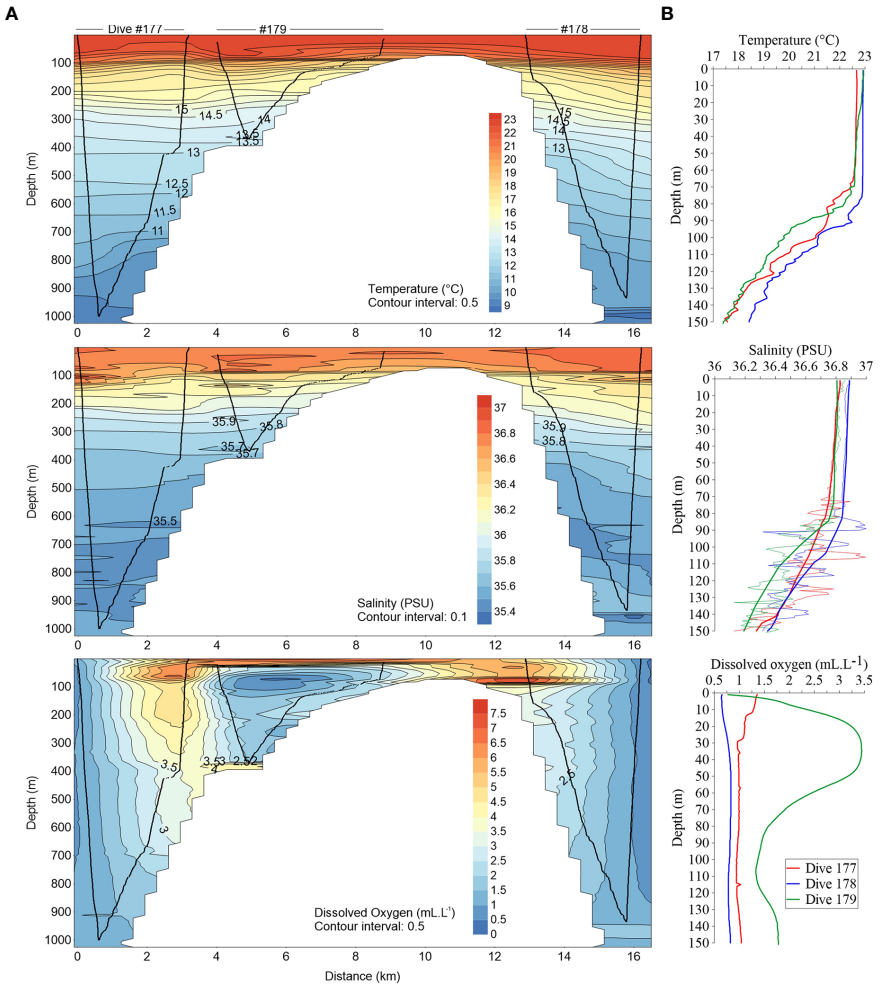

FIGURE 2
(A) Cross-sectional distribution of water temperature, salinity and dissolved oxygen concentration from the along-ridge water column profiling dives (western to eastern flank) with the sub-mounted CTD (downcast, along seabed and upcast); **(B)** Downcast vertical profiles of those parameters until 150 m depth. At salinity plot solid tick lines represent general trend and thin lines *in situ* measurements.

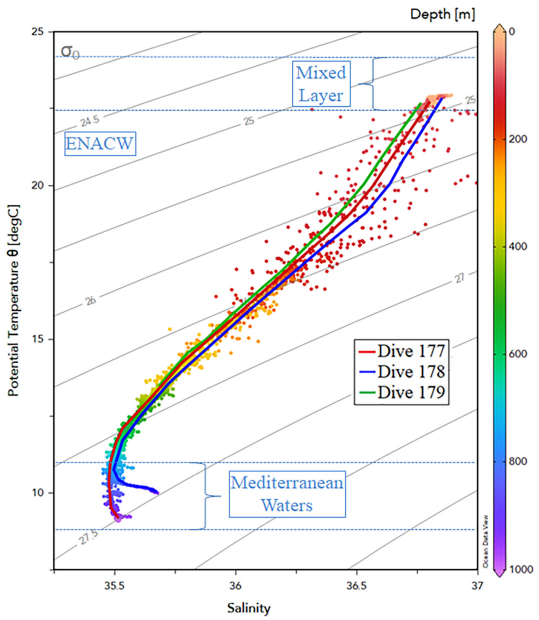

FIGURE 3
Temperature-Salinity (T-S) diagram for the three stations surveyed (#177, #178, and #179) with indication of water mass structure. The Mixed Layer Depth, East North Atlantic Central Water (ENACW) (σ_θ ranges from 26.50–27.30 kg.m^{-3} according to Liu and Tanhua, 2021) and Mediterranean waters are indicated within blue dashed lines.

(ENACW). Below 750 m depth, a sudden increase in salinity with a maximum (35.68) at the bottom (935 m depth), suggests the influence of Mediterranean water (Figure 3).

The nutrient distribution in the water column increased with an increasing depth gradient (Table 1). The highest concentrations of dissolved inorganic nitrogen (DIN, ~19.09–10.99 µM), phosphate (~1.79–0.43 µM) and silicate (~4.00–1.11 µM) were recorded at the maximum depth surveyed for all dives. Nutrients were found at low concentrations in the mixed water layer. The near surface DIN (~1.79 µM) and silicate (~0.19 µM) concentrations were higher at the WFS area (#179) while phosphates were higher in areas more distant from the ridge crest (western side: ~0.27 µM and eastern side: ~0.43 µM). Except for the deepest area (334 m depth) surveyed in the WFS transect (25.00), the N:P ratio was always less than 16, referenced value (Redfield, 1934). Also, the near surface N:P ratio was higher (10.78) than at the potential DCM layer (4.56) around 85 m depth in that transect compared to the other two areas investigated (WF and EF) where a negative trend from deeper to shallow depths was found.

TABLE 1 Dissolved inorganic nutrient concentrations (µM) measured at the Madeira-Desertas Ridge: phosphate (PO_4^{3-}) silicate [$Si(OH)_4$], dissolved inorganic nitrogen (DIN = nitrate + nitrite) and Redfield ratio N:P.

Location (dive number)	Depth (m)	PO_4^{3-} (µM)	$Si(OH)_4$ (µM)	DIN (µM)	N:P
Western flank (#177)	980	1.62	4.00	19.09	11.79
	64	0.25	0.44	2.35	9.53
	4	0.27	0.09	0.65	2.39
Eastern flank (#178)	935	1.79	3.27	14.43	8.06
	69	0.51	0.31	2.30	4.55
	7	0.43	0.05	1.17	2.73
Western flank towards the summit crest (#179)	334	0.43	1.11	10.99	25.50
	85	0.21	0.11	0.94	4.56
	15	0.17	0.19	1.79	10.78

Monthly mean of satellite-based images showed biophysical properties within the ridge different from the surrounding waters. This area had colder surface waters (0.3 to about 0.8°C less, Figure 4A) with higher concentrations of chlorophyll-α (almost 0.1 vs 0.06 mg.m-3 or less, Figure 4B) and dissolved oxygen (4.99 vs 4.95 mL.L^{-1} Figure 4C). The sea surface salinity (SSS) was slightly higher (36.78 vs 36.75, Figure 4D), the sea surface height (SSH) was lower (-0.095 m vs -0.085 to -0.058 m, Figure 4E), the volume attenuation coefficient of downwelling radiative flux in seawater at 490nm (Kd_{490}) was higher (0.033 vs 0.025 m^{-1}, Figure 4F), the coloured dissolved organic matter (CDOM) was slightly higher (ca. 0.033 at the ridge and 0.035 to 0.1 in coastal waters of Madeira island vs 0.024 m^{-1} in open ocean waters, Figure 4G), and the Secchi disk depth (Zsd, an indicator of turbidity) was a bit lower (ca. 29.5 m vs 31.2 m in deeper waters around the ridge, Figure 4H). Mean currents were mostly flowing south westwards (i.e., eastward, and northwards velocities of ca. -0.22 m.s^{-1} and -0.23 m.s^{-1}, respectively; Figures 4I, J). Mean seawater surface velocity was higher than in vicinity areas showing values around 0.31 m.s^{-1} (< 2.0 m.s^{-1}, Figure 4K). By contrast, values of significant wave heights were lower in the ridge (from 1.6 to 1.8 m), and in general, in the southeastern coast of the Madeira Island (Figure 4L). Mean wave periods ranged from 11 to 12 s (Figure 4M). The dominant wave direction was mainly from the south (with waves approaching from within the segments 150° to 220° approximately, Figure 4N). We have also detected a cyclonic-like vortice structure positioned at the ridge (Figure 4).

Seabed substrates and topography

The seabed observed along the submersible dive had a varied terrain with parts of steep, rugged bedrock at depths between 366 and 150 m, more level parts with sand overlying bedrock at depths between 150 and 120 m and patches of exposed bedrock with a crust of live coralline algae (cf. *Lithophyllum incrustans*) shallower than 120 m depth (Figure 5). Level seabed dominated by maërl (free-living, non-geniculate coralline algae) and sand was the dominating substrate below and between rocky outcrops shallower than 120 m depth. Overall, the dominating substrate in terms of percentage surface cover consisted of sand overlaying the basaltic bedrock, covering up to 75% of the seabed in the

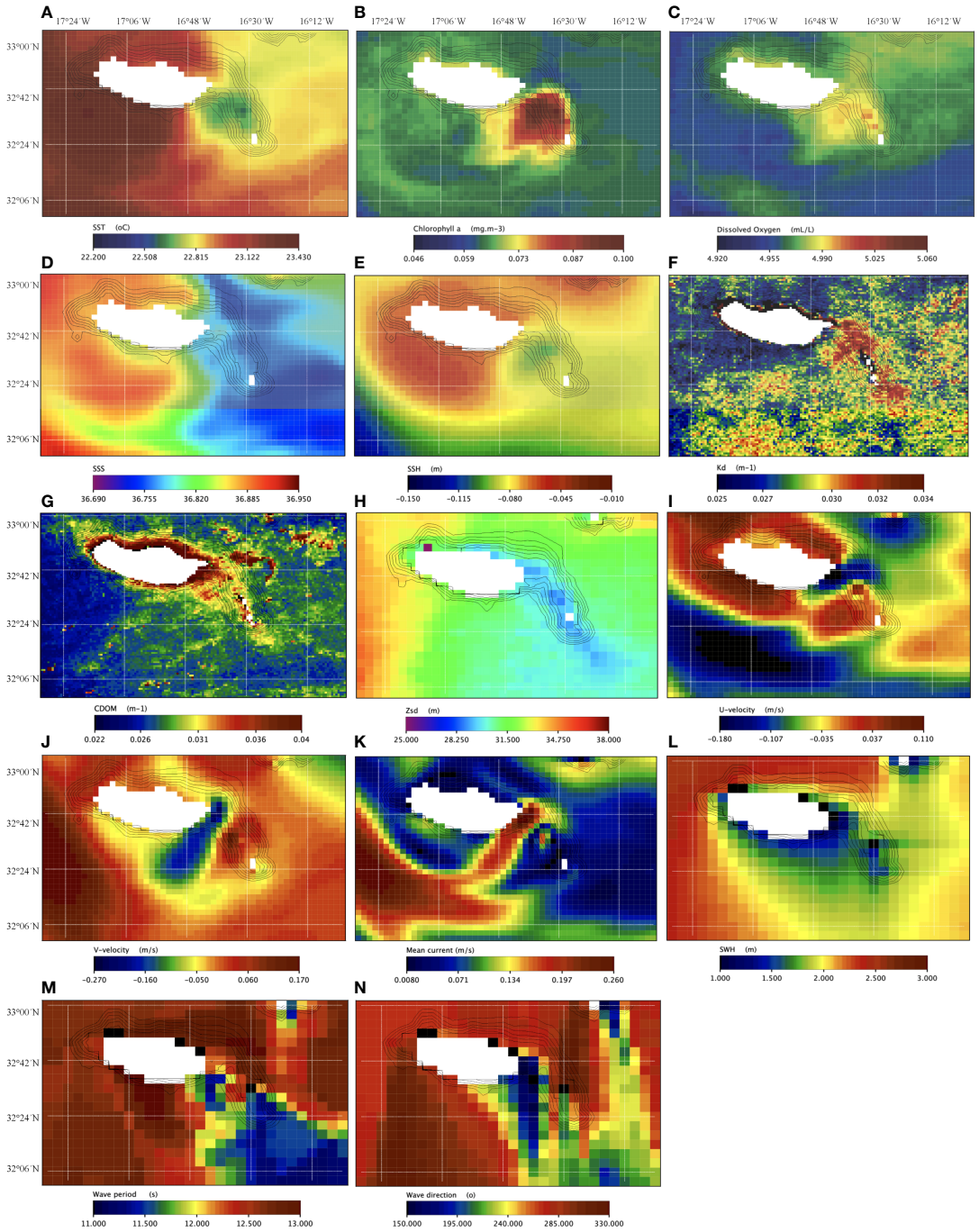

FIGURE 4
Monthly mean MODIS/AQUA-derived products for the Madeira archipelago: **(A)** sea surface temperature (SST, in °C); **(B)** chlorophyll-α (mg.m^{-3}); **(C)** dissolved oxygen (mL.L^{-1}); **(D)** sea surface salinity (SSS, in PSU); **(E)** sea surface height (SSH, in m); **(F)** volume attenuation coefficient of downwelling radiative flux in seawater at 490nm (Kd_{490}, in m^{-1}); **(G)** coloured dissolved organic matter (CDOM in m^{-1}); **(H)** Secchi disk depth (Z_{sd}, in m); **(I)** eastwards sea surface water velocity (u-velocity, in m.s^{-1}); **(J)** northwards sea surface water velocity (v-velocity, in m.s^{-1}); **(K)** mean current (in m.s^{-1}); **(L)** significant wave height (SWH, in m); **(M)** wave mean period (s); and **(N)** mean wave direction from north (°).

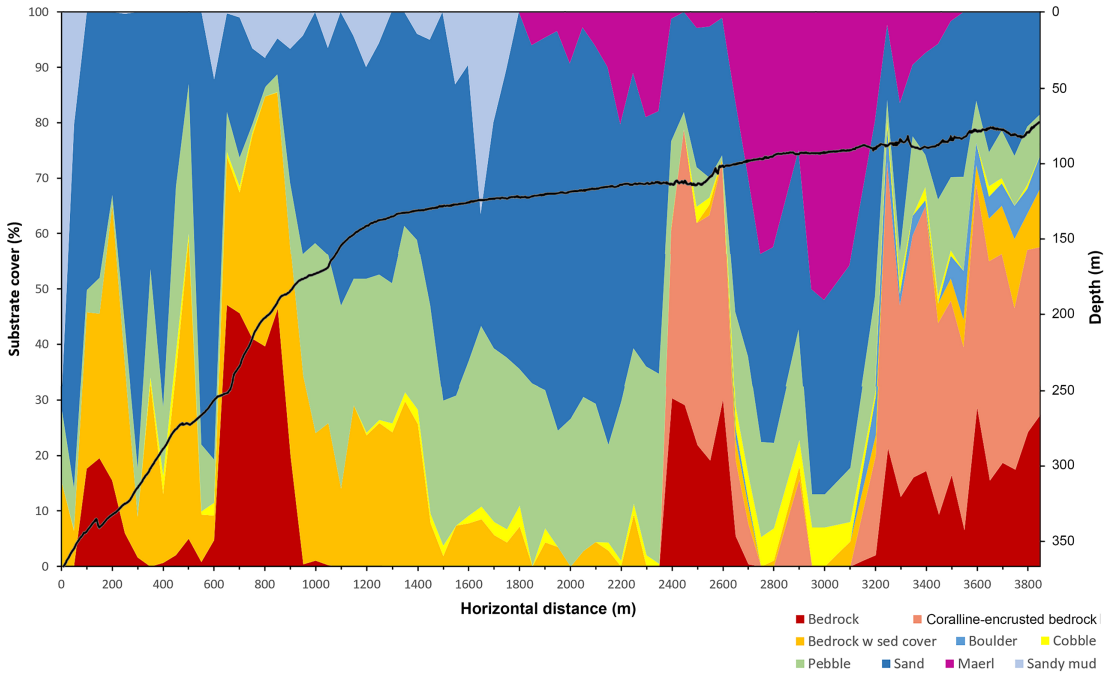

FIGURE 5
Depth profile (solid line) along the transect surveyed with the submersible LULA1000 and composition of substrate types shown as percentage seabed surface cover (estimated as average percentage within 50m video samples).

video samples. In the deep, steep parts, dominated by exposed bedrock at depths between 240 and 180 m, the angle of the seabed was ca. 10° on average but could exceed 45° locally. Sand and gravel commonly occurred in patches on ledges and terraces. Sandy mud occurred mainly in the deepest part around 366 to 350 m and patchily on flat stretches around the break between 130 and 150 m. The patchiness of sand, pebble and sediment-covered bedrock between 200 and 300 m depth is reflected as a spiky pattern in Figure 5. At the summit of the ridge, there were areas of sand and pebble between patches of exposed bedrock. The coralline algae covered between 30 and 50% of the seabed on average within the 50 m long video samples. Locally, at a meter scale it often covered 100% of the hard substrate.

Taxonomic richness and species abundance

In total, 102 taxa were observed, of which 59% were identified to genus or species level and the remaining were assigned to OTUs (Supplementary Table S2). The vast majority were sessile organisms (73.5%), and fishes were the most represented group among the mobile fauna (70%). The three most taxa-rich classes were Demospongiae (27 taxa; 7 families), followed by Anthozoa (24 taxa; 11 families), and Actinopterygii (17 taxa, 6 families). Of the Anthozoa, Alcyonacea (soft corals and gorgonians) was the most diverse group (13 taxa, 6 families). Antipatharia (black corals) comprised nine taxa and three families. Scleractinia (stony corals) and Zoantharia were each represented by only one taxon.

The flora was dominated by Rhodophyta (11 taxa; 7 families). The Phaeophycea and Chlorophyta were poorly represented (one taxon). The majority of the Rhodophyta belonged to the class Florideophyceae and were assigned to morphotypes described as the species they reminded most (e.g., Florideophyceae cf. *Kallymenia reniformis*). Fifteen of the sponges OTUs (53%) could not be designated to a taxonomic level lower than Class but were described as different morphotypes. The fish fauna identified to species level (11 spp.) were represented mainly by demersal species spanning 6 families and 11 genera. The family Labridae was represented by four taxa (*Bodianus scrofa* and *Coris julis* were identified to species).

In addition, four new species are here reported for the first time to Madeira: the alcyonacean gorgonians *Dentomuricea* aff. *meteor* (family Plexauridae) and *Paracalyptrophora josephinae* (Primnoidae); the antipatharian coral cf. *Distichopathes* (Aphanipathidae); and the brown algae *Laminaria ochroleuca* known as the "golden kelp" (Figure 6, MADM 7125; Supplementary S3: GenBank accession numbers ON951970 and ON951971).

FIGURE 6
Morphology of an adult plant of *Laminaria ochroleuca* (MADM 7125) photographed immediately after collection with the Lula1000 submersible. Scale: 40 cm.

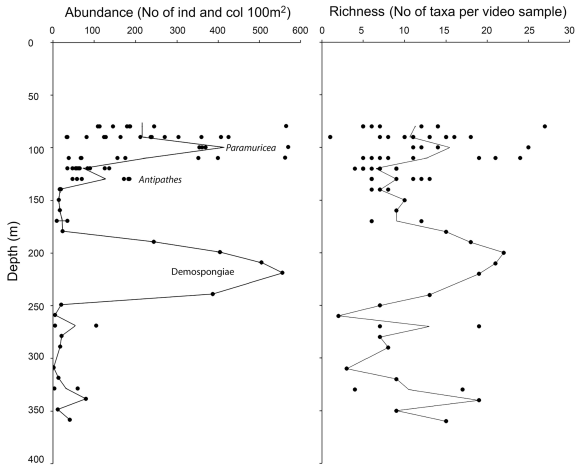

FIGURE 7
Bathymetric distribution of abundance (individuals and colonies per 100 m^2) and taxa richness for the 50m video samples. Peak abundance for *Paramuricea* cf. *grayi*, *Antipathes* sp. and sponges (Demospongiae) is indicated. Mean values are indicated with a line.

Despite 32 taxa were only observed once among the 78 video samples examined (i.e., in one video sample), 24 of them were recorded with more than 100 individuals or colonies. In total, 19 989 colonies and individuals were counted, of which the most common taxa recorded with > 500 individuals or colonies were *Antipathes* sp. (4921 colonies), small (<5 cm) Demospongiae Indet. (1340 colonies), *L. ochroleuca* (1013 individuals), *Pachastrella monilifera* (643 colonies), small yellow-bright digitiform Demospongiae cf. *Pseudotrachya hystrix* (548 colonies), and Axinellidae Indet. (508 colonies). We found two peaks in taxonomic richness and abundance along the depth gradient (Figures 7, 8): one narrow at shallow depths (80–120 m, up to 27 taxa) followed by a wider and deeper one around 180–250m (up to 22 taxa). In terms of maximum abundances of colonies or individuals per 100 m^2, values reached 571 and 556 for the shallower and deeper peaks, respectively.

Bathymetric zonation and biotopes

Six main zones of benthic communities were observed (Figures 9, 10). In general, these were characterised by astrophorina and axinellid sponges, and coral gardens populated by several alcyonacean gorgonians and antipatharians that exhibited a variety of morphologies (whip to feather-like, flabellate, bushy and bottle brush) below 130 m depth.

Above that depth, macroalgal dominance was clear, including dense stands of *L. ochroleuca*, maërl and other crustose coralline species, co-occurring with antipatharian corals (e.g., *Antipathes* sp., *Stichopathes* sp., *Antipathella wollastoni*) and large hydroids. These results were also reflected by TWINSPAN (Table 2) and DCA ordination (Figure 11), which revealed six main classes of video samples with characteristic taxa, hereafter called biotopes. Loose kelp plants were observed scattered in low density at depths between 125 and 273 m. These were not included in the ordination analyses as they have been dislodged and transported away from their habitat.

These biotopes, along with indicator species for each, were identified after up to three divisions performed by TWINSPAN (two divisions: biotope 1 and 2, three divisions: biotopes 3-6) and separated well above the gradients analysed in the DCA ordination (Figure 11). The total variance ("inertia") in the species data was 3.3004. Most of this variance was explained by the first DCA axis. The first axis was strongest correlated with depth (r=0.98), salinity (r=-0.94), and temperature (r=-0.90), whereas the second axis was correlated strongly with the percentage cover of *Lithophyllum*-covered bedrock (r=0.82), exposed bedrock (r=0.66), and pebble (r=-0.61).

Biotope 1 – Mixed *Viminella* and sponge garden on exposed rock on deep slope (Figures 9, 10A). This biotope consisted of 13 video samples, comprising 9.6 taxa on average per sample (range interval = 2–19, total observed = 37). Biotope 1 was located in the deepest part of our survey (252–366 m) and the seabed was dominated by sand and bedrock partly covered

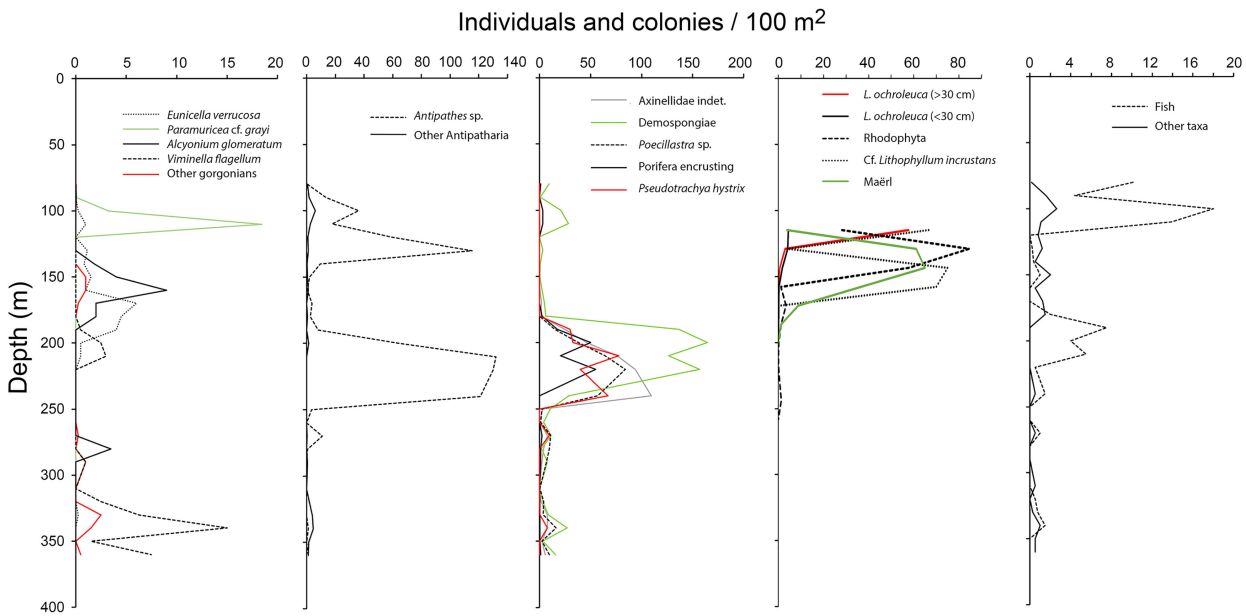

FIGURE 8
Bathymetric distribution of the abundance of dominant taxa. *Lithophyllum* and maërl is represented as percentage coverage.

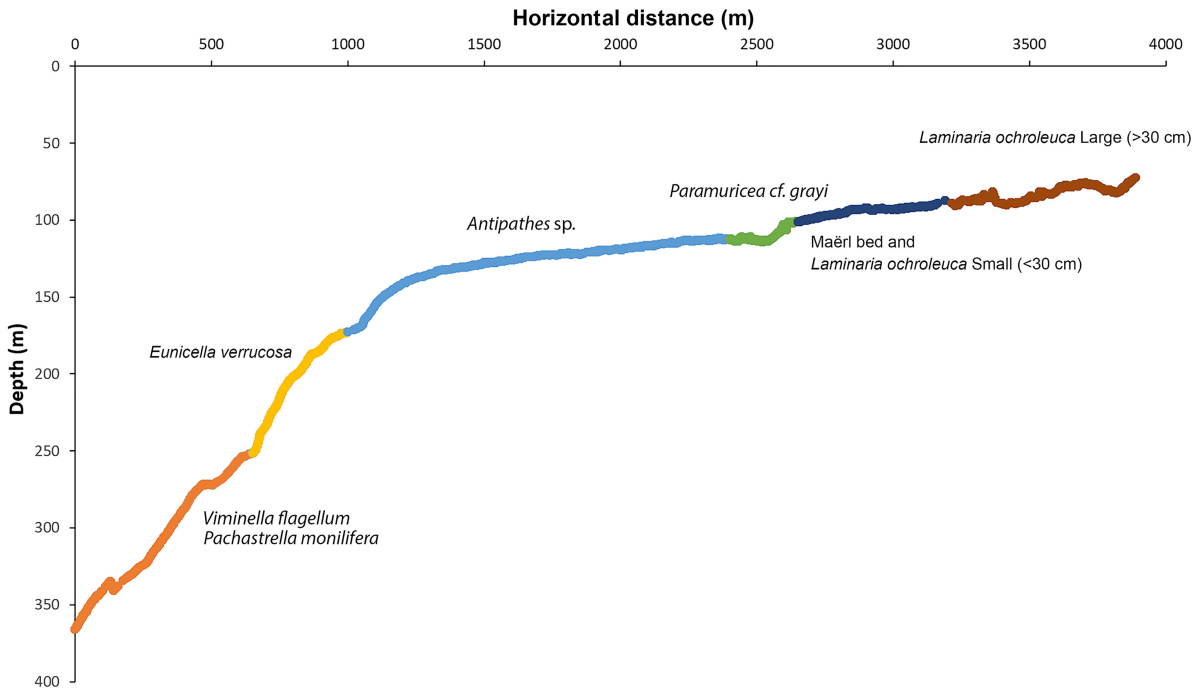

FIGURE 9
Distribution of video samples along the depth gradient explored in the Madeira-Desertas Ridge classified as six biotopes, with characteristic species identified with TWINSPAN. Biotope 1 (orange) – Mixed *Viminella* and sponge garden on exposed rock on deep slope; Biotope 2 (yellow) – *Eunicella* garden on exposed rock on upper slope; Biotope 3 (light blue) – *Antipathes* garden on level sandy bottom; Biotope 4 (green) – *Paramuricea* garden on coralline-encrusted bedrock; Biotope 5 (dark blue) – Maërl bed; Biotope 6 (brown) – Kelp forest.

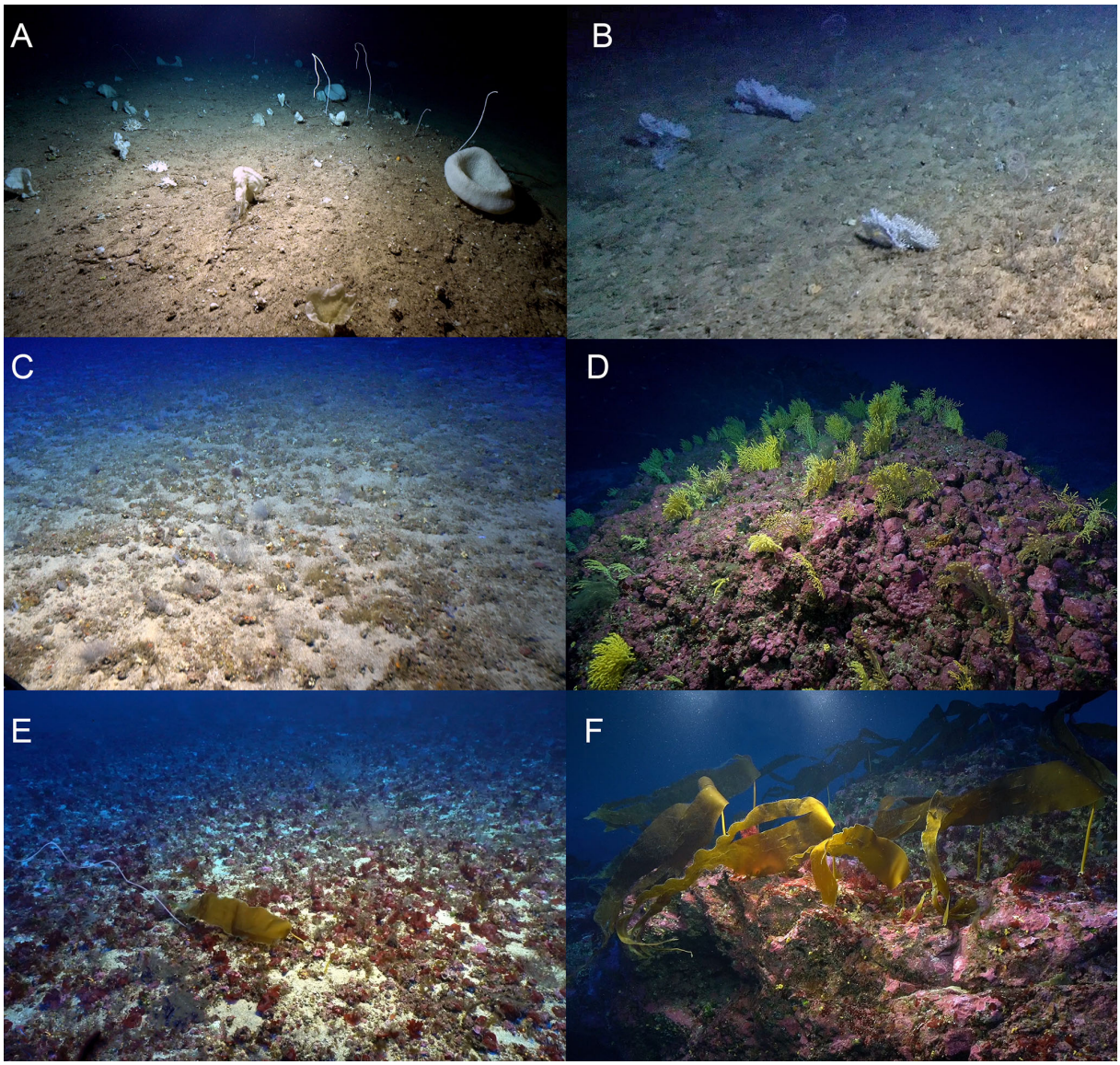

FIGURE 10
Examples of the six biotopes found at the Madeira-Desertas Ridge: aphotic **(A,B)**, ecotone **(C)** and mesophotic ecosystems **(D–F)**. **(A)** Mixed *Viminella* and sponge garden, here with *Viminella flagellum*, *Asconema setubalense*, astrophorina *Pachastrella monilifera*, and various demosponges; **(B)** *Eunicella* garden; **(C)** *Antipathes* sp. garden on level sandy bottom; **(D)** *Paramuricea* garden; **(E)** Maërl bed with small (juvenile) *Laminaria ochroleuca*; and **(F)** *L. ochroleuca* forest.

with a layer of sediment. The alcyonacean gorgonians *V. flagellum*, *D.* aff. *meteor* and *P. josephinae* as well as a variety of sponges in moderate densities (10–20 colonies per 100m^2) were the characteristic megafauna. Of these three gorgonians, *V. flagellum* was the most abundant species with a mean density of 4.8 colonies per 100m^2 for the 50 m video samples (max. = 15 colonies per 100m^2). Locally (at the scale covered by a video frame), it was observed with a maximum density of ca. 40 colonies per 100 m^2. The tall primnoid *P. josephinae* was only found in this biotope occurring in low densities (mean = 0.4; max. = 2.5 colonies per 100m^2) and was identified as an indicator species by TWINSPAN. The astrophorina sponge *P. monilifera* was abundant (mean = 6.6, max = 21), while most other sponges occurred with relatively low abundance and were not possible to identify to a low taxonomic level. These were represented by axinellid sponges, a foliose morphotype and colonies of the genus *Polymastia* (Polymastiidae).

Biotope 2 – *Eunicella* garden on exposed rock on upper slope (Figures 9, 10B). This biotope includes seven video samples from the upper part of the surveyed slope at depths

10.3389/fmars.2022.973364

TABLE 2 Characteristic taxa and range of environmental conditions for the six biotopes identified with up to three divisions by TWINSPAN.

	Twinspan group					
	1	**2**	**3**	**4**	**5**	**6**
Biotope name	Mixed *Viminella* and sponge garden on exposed rock on deep slope	*Eunicella* garden on exposed rock on upper slope	*Antipathes* garden on level sandy bottom	*Paramuricea* garden on coralline-encrusted bedrock	Maërl bed	Kelp forest
No of samples	13	7	28	5	11	14
Depth (m)	305 (253-366)	203 (173-252)	128 (112-173)	110 (101-114)	94 (88-101)	83 (72-91)
Dominating substrate	Sand	Bedrock	Sand	*Lithophyllum* -encrusted bedrock	Maërl	Coralline-encrusted bedrock
Sub-mounted CTD (along bottom)	**Oceanographic variables:**					
Oxygen (%)	27.9 (25.5-32.3)	37.9 (26.1-45.9)	37.2 (34.9-39.9)	34.5 (33.6-37.1)	35.8 (34.6-39.2)	47.7 (36.9-66)
Temperature (°C)	13.9 (13.4-14.6)	15.8 (14.6-16.3)	17.2 (16.3-18.0)	18.1 (18.0-18.2)	18.3 (18.1-19.0)	20 (18.6-21.1)
Salinity (PSU)	35.8 (35.7-35.9)	36.0 (35.8-36.1)	36.2 (36.1-36.3)	36.3 (36.3-36.4)	36.4 (36.3-36.4)	36.5 (36.4-36.6)
	Seabed substrates (% cover):					
Sandy mud	8	5	4	0	0	0
Sand	50	19	51	23	35	23
Pebble	12	7	28	6	14	10
Maërl	0	0	4	2	38	4
Cobble	1	0	1	1	5	1
Boulder	0	0	0	0	1	4
Bedrock w sediment cover	24	34	11	1	2	5
Exposed bedrock	6	34	0	26	1	17
Coralline-encrusted bedrock	0	0	0	41	5	36
No of taxa	10 (2-19)	16 (6-22)	8 (4-13)	19 (7-25)	12 (7-16)	11 (5-27)
No of ind. and col. 100 m^{-2}	29 (2-105)	308 (23-556)	77 (10-185)	396 (156-563)	268 (35-407)	206 (34-566)
Tot No of taxa	37	39	34	36	30	36
Characteristic taxa	*Viminella flagellum, Pachastrella monilifera*, *Dentomuricea* aff. *meteor*	*Eunicella verrucosa*	*Antipathes* sp.	cf. *Lithophyllum incrustans*	Maërl, *L. ochroleuca* (<30 cm)	*Coris julis, Nemertesia ramosa*
Indicator taxa	*Paracalyptrophora josephinae*	cf. *Pseudotrachya hystrix*	*Alcyonium glomeratum*	*Paramuricea* cf. *grayi*	cf. *Callophyllis* sp.	*L. ochroleuca* (≥30 cm)

between 173–252 m, just below a marked break to the level shelf above. The seabed was dominated by both exposed bedrock and bedrock with a sediment cover. It represents the biotope with the highest taxonomic richness (39 taxa) with a mean of 16 taxa per video sample. In terms of megafaunal abundance, it had an averaged number of 308 individuals or colonies per 100 m^2, pointing to high abundances in that area, partly explained by the high densities of the antipatharian coral *Antipathes* sp., and the demosponges *P. monilifera*, small yellow-bright digitiform Demospongiae cf. *P. hystrix* and an unidentified Axinellidae. Most characteristic for this class was the temperate alcyonacean gorgonian *E. verrucosa* (Gorgoniidae) occurring with up to 12 colonies per 100 m^2 (mean = 3.1). The TWINSPAN identified the small yellow-bright digitiform Demospongiae cf. *P. hystrix* as an indicator species of this biotope, occurring with up to 78 colonies per 100 m^2.

Biotope 3 – *Antipathes* garden on level sandy bottom (Figures 9, 10C). This biotope represented the largest group separated by TWINSPAN with 28 video samples from the outer part of the level shelf at depths between 112 and 173 m depth. The seabed consisted mainly of sand and pebble. On average it had a relatively low taxonomic richness (mean = 8

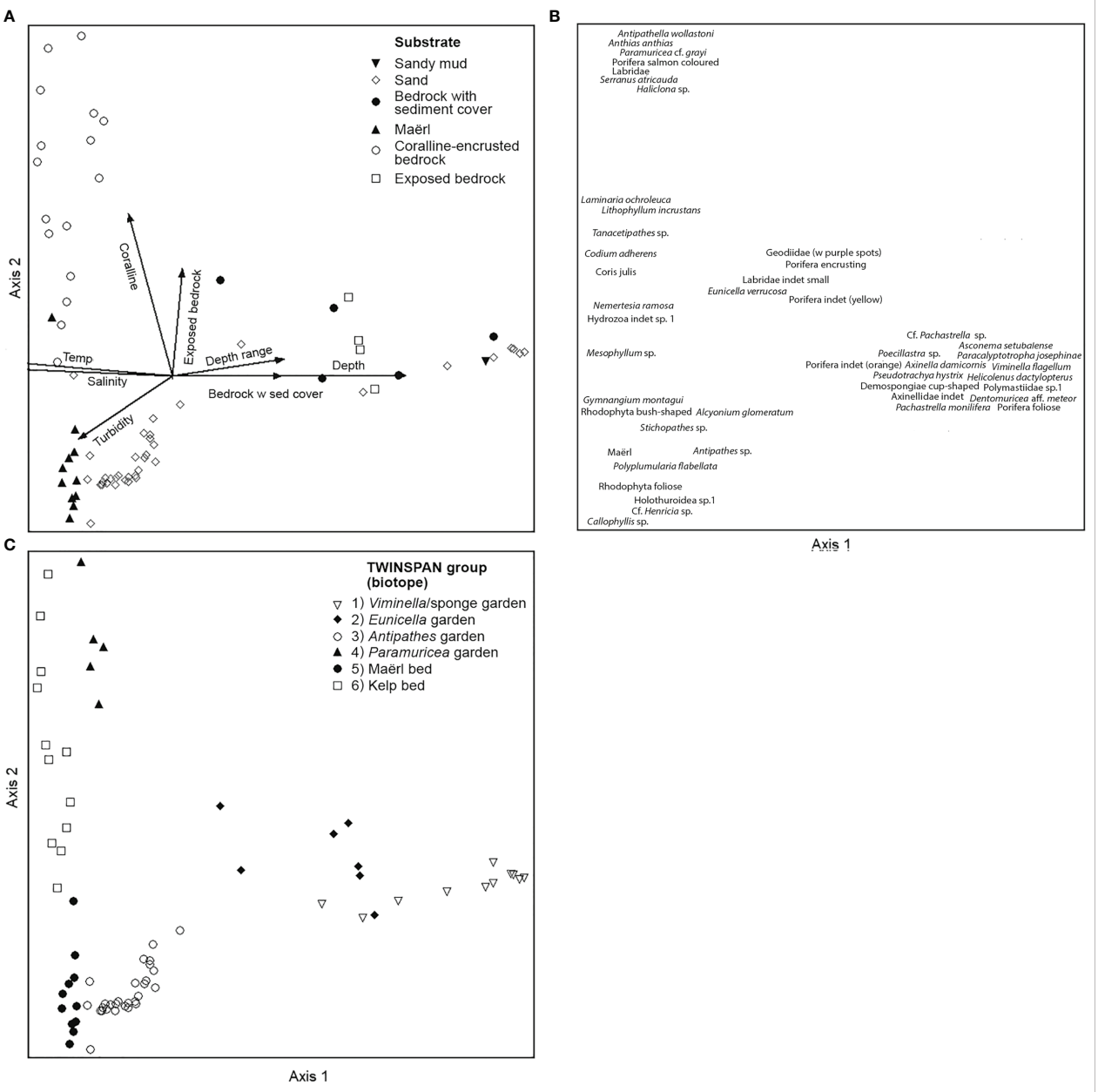

FIGURE 11
DCA plots from analysis of quantitative data (operational taxonomic units [OTU] and environmental factors) of 74 video samples, 48 OTU, and 21 environmental variables. **(A)** Biplot of samples (classified according to dominating substrate of the sample) and environmental factors shown as arrows (only factors with r > 0.4 are shown). **(B)** Species plot. **(C)** Plot with samples classified according to the result of TWINSPAN analysis of the same material.

taxa per video sample) with a maximum of 13 taxa per video sample. The mean abundance of 77 individuals or colonies per 100 m^2 was mainly caused by relatively high densities of *Antipathes* sp., which was visually the most characteristic species of this biotope. Its taxonomic status is currently under debate requiring further investigation and additional genetic data (A. Braga-Henriques and D. Opresko, pers. comm.). The alcyonacean soft coral *Alcyonium glomeratum* was identified as indicator species. It was typical but occurred with low densities (mean = 0.7 colonies per 100 m^2). This TWINSPAN class should be interpreted as an ecotone, i.e., a transition area between mesophotic and "aphotic" communities as it had a few occurrences of various bushy red algae starting around ca. 120 m depth.

Biotope 4 – *Paramuricea* garden on coralline-encrusted bedrock (Figures 9, 10D). This was the smallest class identified in the multivariate analysis consisting only of five video samples at depths between 101 and 114 m. The temperate alcyonacean gorgonian *Paramuricea* cf. *grayi* was the indicator species in TWINSPAN. Approximately 41% on average of the seabed was bedrock covered with calcareous red algae (cf. *Lithophyllum incrustans*). The remain areas consisted of exposed bedrock, i.e., without the cover of encrusting coralline algae (26%) and seabed surfaces covered by sand in the deeper parts between the hummocky bedrock (23%). Considering the reduced number of samples and the high taxonomic richness (36 taxa), our results point to a highly diverse biotope, with a mean number of taxa of 19 and maximum of 25 taxa per video sample. We found average densities of *P.* cf. *grayi* of 30.8 colonies per 100 m^2 and maximum values of 53.8 colonies per 100 m^2 in this biotope.

Biotope 5 – Maërl bed (Figures 9, 10E). Eleven samples were clustered for this biotope that occurred at depths between 88 and 101 m. Maërl and sand covered most of the seabed in flat depressions between rocky outcrops (73%), where sand and maërl accumulate. Apart from the maërl, most characteristic for this biotope was small (<30 cm) plants of *L. ochroleuca* and bushy red algae (cf. *Callophyllis* sp.). However, *Antipathes* sp., *Stichopathes* sp., *Polyplumularia flabellata* (Hydrozoa) and smaller brown (Phaeophyceae) and red (Rhodophyta) algae were common.

Biotope 6 – Kelp forest (Figures 9, 10F). This biotope was represented by 14 video samples at depths between 72 to 91 m and showed a high taxonomic richness with up to 27 taxa per video sample. The seabed was dominated by bedrock, mainly coralline encrusted algae. Characteristic for this biotope was the kelp *L. ochroleuca* identified as indicator species by TWINSPAN. We found a population with large kelp plants (maximum stipe lengths of approximately 70 cm) at around 80 m depth. Several red algae taxa occurred in high abundance between the kelp plants. The labrid fish *C. julis* and hydroid colonies of *Nemertesia ramosa* were common. The mean abundance for all taxa estimated for the video samples was of 118.7 individuals per 100 m^2 mainly represented by *L. ochroleuca* and various red algae. The density of kelp plants increased with decreasing depth, and the highest densities with up to ca. 100 kelp plants per 100 m^2 were observed between 73 and 87 m depth extended over a distance of 350 m (Figure 7). The patchiness of the kelp plants reflected the distribution of stable rocky substrate. Since these densities represent estimates aggregated over 50 distances, the patchy distribution of the kelp with much higher local densities (up to 3 per m^2) is not reflected in this figure. Several turf forming red algae were observed on the seabed between the kelp plants. Characteristically for *L. ochroleuca*, no epibionts were observed on the stipe or haptera. However, short hydrozoan colonies were seen on several specimens colonising the lamina. The sea urchin *Arbacia lixula* was recorded in low numbers inside and outside the kelp forest, but no signs of moderate to severe grazing on kelps were observed.

Physical environment of biotopes and their characteristic taxa

Except for the shallowest biotopes (kelp forest, maërl bed and *Paramuricea* garden) their range in depth and temperature did not overlap (Table 2). The deepest (253–366 m) and coldest (13.4–14.6°C) biotope was "Mixed *Viminella* and sponge garden on exposed rock on deep slope". Within biotope 6 (Kelp forest) the temperature was between 18.6 and 21.1°C, and the salinity ranged from 36.4 and 36.6. There was a positive correlation between oxygen content and kelp density. In the high density patches the oxygen saturation was from 44 to 66%, whereas in patches with low densities the saturation was from 34.8 to 52%. Estimates from satellite imagery on the percentage of 490 nm radiation (FR_{490}) at the kelp forest and maërl biotopes indicate values ranging from 9.3–4.9% and 3.5–2.3%, respectively.

Shallower than 130 m, the hydrodynamic regime was influenced by wave-induced water motion. The intensity of the waves increased from 130 m up to the shallow (70 m) end of the transect. The water motion was clearly observed (and strongly felt inside the sub) as the kelp plants were alternating, bending from one side to the other. Bottom currents near those plants mainly had a direction of 145°, towards south-east (Figure 12). The waves moved the lamina perpendicular to this direction,

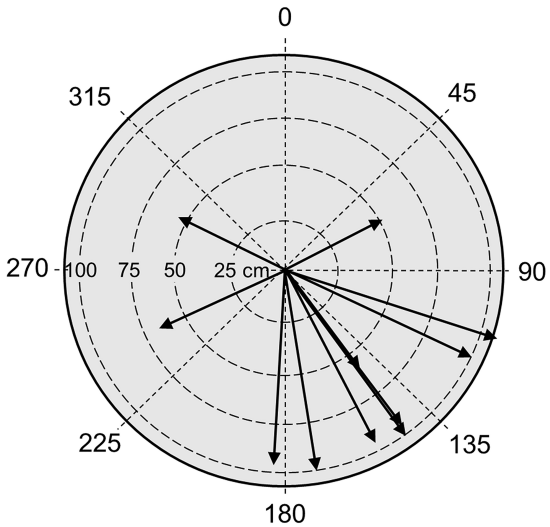

FIGURE 12
Bottom currents and wave action in the kelp forest. The direction of the arrows indicates the mean direction of the *Laminaria ochroleuca* blades (lamina) during wave movement. The length of the arrows indicates the distance the tip of the blades that were moved by the waves.

meaning that the waves were rolling back and forth northeast-southwest. The period of the waves (i.e., the time from the lamina started moving from one side until it returned back to its starting point on the same side) was very stable between 12 and 16 s (mean value = 13.8 s). The average wavelength was 156 cm.

Associated fish fauna

At the deepest zone (355–170 m), we found the school shark *Galeorhinus galeus* three times swimming vigorously in front of the sub and ca. 1m above the seabed. This is a semi-pelagic demersal species well-known for its high mobility. Along the dive, a number of other species were recorded (Supplementary Table S2), including sedentary species of commercial value (e.g., the blacktail comber *Serranus atricauda* and the blackbelly rosefish *Helicolenus dactylopterus*). At upper depths (<130 m), schools of small Indet. Labrid fishes became frequent observations. In the kelp and gorgonian (*Paramuricea*) biotopes, small fishes, adult and juveniles, were quite abundant (e.g., *Anthias anthias*, small Indet. Labrids, *C. julis*), providing further evidence of these hotspots as providers of habitat, refuge and spawning grounds. Several *S. atricauda* were seen chasing *A. anthias*, which could be interpreted as a predation trait behaviour.

Signs of fishing impact

Lost fishing gear (monofilament lines) were observed 17 times across the investigated area at depths between 337 and 113 m. Damaged megafauna were represented by alcyonacean gorgonians with 8.8% of the colonies showing evident mechanical impacts (Figure 13). The majority of these observations (14) were made in the *Paramuricea* biotope with lines entangled in colonies and suspended on the rocky bottom over distances between 2 to ca. 5 m. We found damaged *P.* cf. *grayi* on all occasions where lost fishing gear occurred. In total, 17 colonies of *P.* cf. *grayi* were damaged at depths between 102 and 113 m. Nine of these had broken branches, eight had clear tissue damages while three colonies had both. Two of the damaged colonies were infested with small hydrozoans. Twenty-three (25%) *V. flagellum* colonies showed different signs of damage: eleven with impact-induced side branches, nine with tissue damage (parts with naked tissue), and two with broken skeleton. These occurred between 325 and 337 m depth. One colony was colonised by small hydrozoans. Three *P. josephinae* were broken and severely colonised by zoanthids at depths between 324 and 336 m, and three colonies of *E. verrucosa* were also broken and colonised with epibionts (113-133 m). Three colonies (33%) of *D.* aff. *meteor* showed signs of impact: one was broken (333 m), one was covered with hydrozoans (329 m), and one at 300 m depth had tissue injured.

Discussion

Megabenthic diversity

We found complex benthic communities (> 100 taxa) dominated by different species of great conservation value and ecosystem functioning, some new for Madeira or poorly known requiring *in situ* image data.

The new records of *L. ochroleuca* fill out a previously widely open gap in the oceanic regions between Morocco and the central Mid-Atlantic Ridge (20–10°W) and represent by far the deepest (124 m) occurrence of this genus in the northeast Atlantic (Assis et al., 2018). The discovery of maërl at the lower mesophotic zone below 100 m extends far beyond the deepest range of this habitat in the Macaronesian islands of Madeira (Neves et al., 2021: 35 m) and Canary Islands (Otero-Ferrer et al., 2020: ~50 m). The geographical distribution of *D.* aff. *meteor* (VME indicator; ICES, 2020) previously known from the Azores and Great Meteor seamount (Braga-Henriques et al., 2013) is eastwards extended. The eastern and mid-Atlantic range of *P. josephinae* (VME indicator; ICES, 2020) that includes the Bay of Biscay, the Azores, Josephine bank and Atlantis and Great Meteor seamounts is expanded towards the east within the 32-33°N latitude (Cairns and Bayer, 2004). Lastly, this is the first time that high-resolution imagery on a *Paramuricea* population (VME habitat; ICES, 2020) from this region is provided. Unfortunately, voucher specimens were not sampled, which has hampered our identification to species level with a high degree of confidence. Two species of this genus have been reported so far in this region, *Paramuricea grayi* and *Paramuricea hirsuta*, with our population resembling the first. Nonetheless, its presence in Madeira is based on limited material with less than six specimens covering a broad bathymetric range of 125-1968 m (Johnson, 1861; Grasshoff, 1992). Its occurrence in the bathyal zone has also been questioned with most records from the mesophotic zone (Altuna Prados, 1991; Grasshoff, 1992). At the same time, morphological plasticity and sympatry (i.e., overlapping ranges occupying similar ecological niches and habitats) are common traits in temperate congener species leading sometimes to inaccurate identifications (Pica et al., 2018). Therefore, we cannot rule out the presence of a different (or even new) species and thus our identification must be considered as tentative.

Overall, the high number (up to 27) of taxa per video sample across the whole study area reflect an elevated environmental heterogeneity due to the presence of a large submarine ridge feature with potential for localised upwelling (Gove et al., 2016). The higher rate of population differentiation may also be explained by seabed complexity with many substrate classes that can act as physical barriers to connectivity of sessile taxa of specific habitat requirements, or to movement of mobile fauna (Levin and Dayton, 2009). Adding to that, habitat former species

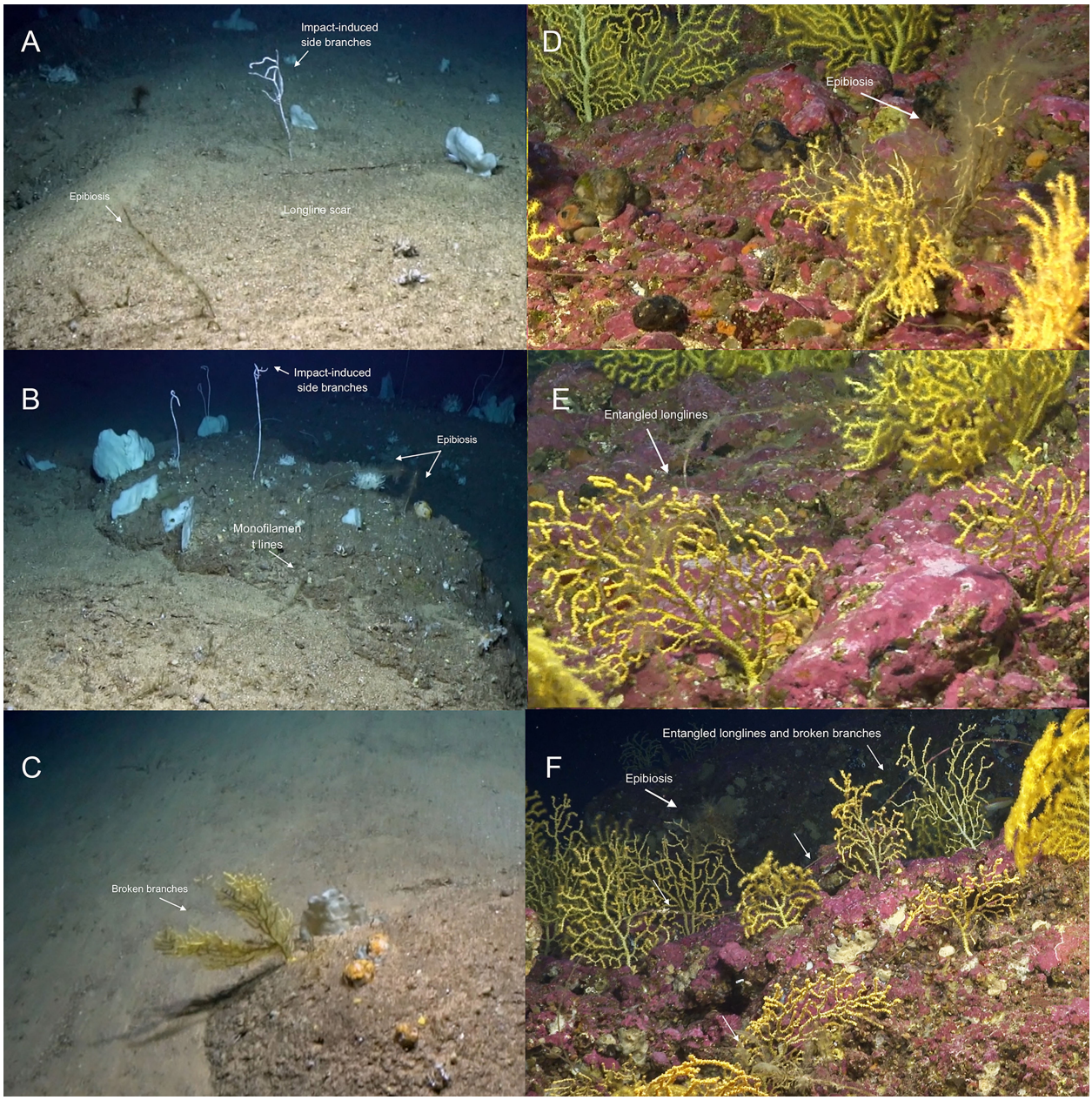

FIGURE 13
Examples of impacted alcyonacean gorgonians. **(A–C)**: from the deep *Viminella* garden, **(D–F)**: from the shallow *Paramuricea* garden.

recognised to facilitate biological productivity in benthic habitats were commonly observed across the whole transect (Thomsen et al., 2010; Cerrano et al., 2010; Ponti et al., 2018).

Nonetheless, the high biological diversity could also be attributed to the "mid-domain effect", where vertical distributions from deep-specialist and shallow species meet due to geometric boundary constraints (Colwell and Lees, 2000; Cerrano et al., 2019). The use of a static depth-range boundary to define mesophotic ecosystems has been previously questioned because communities may shift shallower or deeper depending on local environmental conditions, and thus it should be rather sustained on the loss of shallow (photic) specialist species (Laverick et al., 2017; Lesser et al., 2019). Some authors argued that community break is largely driven by taxonomic turnover and to a lesser degree by ordered species loss along environmental or ecological gradients - nestedness (Stefanoudis et al., 2019). For the study area, the transition zone from mesophotic to "aphotic" could be defined by the gradual loss

of crustose coralline algae (calcareous red encrusting and maërl) from 100 to 125 m depth and the establishment of animal-dominated communities (e.g., sponges and cold-water corals). This depth interval coincides roughly with the upper layers of thermocline, halocline, and consequently, pycnocline. Furthermore, a pronounced transition from shallow to mesophotic was not observed, probably because our survey did not cover areas shallower than 70 m (summit crest), and community turnover, at least for MCEs, occurs around 60 m depth (Lesser et al., 2019).

Benthic zonation in relation to environmental drivers

Our analysis reveals six biotopes with high level of floral and faunal discrimination along the steep environmental gradient related to depth (main driver), as observed by others in deep offshore surveys (Stefanoudis et al., 2019). Due to the type of survey (non-destructive) and sampling methods available, an exact validation of all recorded organisms from each biotope was not possible. Most likely, the number of macroalgal and sponge species will greatly expand when surveys to collect specimens are undertaken but will not change the general description of the community attributes and distribution patterns.

The steepest gradient in temperature (16.8–21.1°C) was found shallower than ca. 130 m depth, while deeper, the temperature differed gradually decreasing from 16.8 to 13.4°C at the deepest part. This bathymetric interval also displays a wide gradient of light attenuation. Unfortunately, it was not possible to undertake light sensor measurements during benthic observations but change in light conditions was clearly observed by the crew on board and also expressed in the gradual occurrence of macroalgae when moving from deep to shallow. In addition to water mass properties (i.e., temperature and salinity) and light attenuation, the substrate composition seems to play a role for habitat provision. The mesophotic biotopes (Kelp forest, Maërl bed and *Paramuricea* garden) occurred shallower than 114 m on solid substrates characterised by maërl and/or bedrock (both exposed and covered by coralline algae). The "ecotone" and "aphotic" biotopes (represented by different coral and sponge species) were found on softer sediments, with contribution of sandy mud and sediment-covered bedrock. This is also the steepest part of the video transect. Seabed slope angle affects sediment abundance and exposure to local currents. Our results indicate that active (sponges) and passive (anthozoans) suspension feeders have a complementary distribution (Figures 8, 9). The occurrence of finer sediments and slower currents is a common feature in the marine environment. The combination of stable substrate and probably higher concentration of fine particulate organic matter may favour sponges in the deep, steep part of the transect.

Top of the ridge

The kelp forest of the upper plain zone (biotope 6) harboured a rich biodiversity providing food and shelter for several species, including labrid fishes (Tuya et al., 2012; Wernberg et al., 2019). It was unexpectedly dense up to ~1 plant/m^2 with individuals clearly profiting from the predominance of exposed bedrock that is critical for attachment, and consequently for successful recruitment (Yesson et al., 2015). Adding to its favourable position below the depth of the mixed surface layer, the thermal seabed regime of 18.6–21.1°C encourages optimal to sub-optimal kelp growth (Franco et al., 2018). According to these authors, when *L. ochroleuca* is exposed to temperatures above 20°C nutrient storage is probably to overcome nutrient-poor periods. Considering previous age estimates for Iberian populations (John, 1969; Drew, 1974), such forest is most likely from 5–7-yr old plants. Since the life cycle of this pluriannual alga can span 7 to 10 years (Drew, 1974) with plants thought to become fertile after 2–6 years (Kain, 1971; Birkett et al., 1998), our observations are from a well-established adult population.

This discovery brings to light Madeira's potential for a climate refugia hotspot for kelps of ocean warming (Graham et al., 2007; Assis et al., 2018). Annual average sea surface temperature is recognised as the most important abiotic variable constraining their distributions (Franco et al., 2018), with recorded values usually ranging from 5 to 25°C, but rarely above 27°C (Jayathilake and Costello, 2020). As such, global trends of increased seawater temperatures have precipitated changes in many species' boundaries (Wernberg et al., 2019). This is the case of *L. ochroleuca* with a range contraction predicted at its southern distributional limit in Morocco (Franco et al., 2018) that corresponds to the same latitude belt of Madeira.

Besides the ridge, overlooked submerged features of the Madeira landscape can also be suited for temperate kelp relict populations such as shallow peak seamounts crossing the euphotic zone. Dense assemblages of *Laminaria rodriguezii* were found at the top of the Vercelli seamount (Mediterranean Sea) at depths from 60–70 m (Bo et al., 2011) and at the summit of Ormond peak (Atlantic Ocean) numerous *L. ochroleuca* plants covered extensive bedrock areas between 20–50 m depth (Ramos et al., 2016).

Light is a fundamental driver for kelp performance with individuals requiring a minimum annual penetration of sunlight (surface irradiance dose) around 40 E m^{-2} (Gattuso et al., 2006). As demonstrated by others, the observation of higher densities of large plants at the kelp forest and lower densities of small plants at the maërl bed (biotope 5) indicates size (and density) stratification with depth as a function of available light on the bottom (Markager and Sand-Jensen, 1992; Gattuso et al., 2006). In *L. ochroleuca* surveys on the Formigas Bank (Azores), the highest densities (kelp forest) occurred between 41.5 and 64.3 m

depth (yearly-averaged percentage of light ranges of 6.0–2.2% FR_{PAR} and 9.5–3.7% FR_{490}) and at lower zones from 47.6 to 81.6 m dense to sparse plants (5.4–0.9% FR_{PAR} and 8.8–1.6% FR_{490}) were seen at the bottom (Amorim et al., 2015). Despite deeper, the new kelp forest was exposed to higher light levels (9.3–4.9% FR_{490}) and 1% of light level was not even achieved at the maërl bed (3.5–2.3% FR_{490}), which reflects well the long-distance range (>100 m depth) of sunlight penetration in the ridge because of the exceptional clear waters in Madeira (Teira et al., 2005). Although kelps can adapt their physiological performance to environmental variation, *L. ochroleuca* is more susceptible to "warmer" habitats than other kelp species such as *Saccorhiza polyschides* (Biskup et al., 2014). Having a less acclimatisation capacity to gradual changes in environment, *L. ochroleuca* tends to occupy a narrower range of physical environments (and rather colder), which is in line with our findings.

Although both kelps and maërl find in current-swept plateaux suitable conditions for growth, including reduced sediment settling, the latter show preference for soft bottoms and can tolerate longer periods of low irradiance (Foster, 2001; Gattuso et al., 2006). As demonstrated by Schubert et al. (2022), maërl show high plasticity to varying light regimes, including maërl from Madeira (*Phymatolithon* sp.). As such, these coralline algae are more adapted to colonise the available soft substrates of the lower plain zone (slight deeper than kelp forest), and in turn, avoid competition with kelps or other organisms attached to the exposed bedrock, abrasion, or even rolling way at the kelp forest. Maërl can also profit from canopy shading of small kelp plants that protect them from detrimental effects of high irradiance (Figueiredo et al., 2000). The presence of bushy red macroalgae in this biotope agrees with taxonomic accounts of associated flora in other areas of the NE Atlantic. According to Peña et al. (2014), 67% of the macroalgae species recorded in maërl habitats are Rhodophyta, and Otero-Ferrer et al. (2020) report that Rhodophyta accounted for the majority of the epiphytic macroalgae taxa (44.4%) followed by Chlorophyta (27.8%) and Ochrophyta (27.8%) in rhodolith beds of Gran Canaria Island (central-eastern Atlantic). As Markager and Sand-Jensen (1992) previously argued there is "an upper zone of mainly leathery algae to about 0.5% surface irradiance (SI), and intermediate zone of foliose and delicate algae to about 0.1% SI".

Nevertheless, the putative absence of *L. ochroleuca* in the surrounding landscape with adequate temperatures, available hard substrates and light for photosynthesis suggests other players, or their combined impact for this discovery off coast (Jayathilake and Costello, 2020). One of those driving forces is likely the terrain slope of the islands. Although this species could profit from the limited annual temperature range of Madeira, surface seawater can reach 23.5°C in summer (monthly average) (Schäfer et al., 2019). This would correspond to the estimated upper lethal boundary (~23–24.6°C) of *L. ochroleuca* sporophytes (van den Hoek, 1982; tom Dieck (Bartsch), 1992; Franco et al., 2018), therefore comprising them to deeper areas where temperatures are cooler, and subsequently to inclined slopes (Quartau et al., 2018). However, the probability for dense forests on those areas is much lower than at the ridge plateau that offers flat areas with surfaces of higher rugosity known to facilitate kelp attachment and spore aggregation (Muth, 2012; Bekkby et al., 2019).

Dispersal ability is a key ecological trait with strong implications for population connectivity and therefore may also provide clues for this confined distribution pattern of *L. ochroleuca* (Lester et al., 2007). Despite its potential for long-distance dispersal (spores or long-lived rafts) of dozens to thousands of kilometres, only 5% go further than 3.93 km (Assis et al., 2018). For that reason, there is a low probability of high densities of spore settlement (the primary dispersive stage) in the coastlines of Madeira and Desertas islands, which negatively affects successful rates of fertilisation and subsequently of sporophyte recruitment (Gaylord et al., 2012). Also, kelp spores have short viability (~1 day; Reed et al., 1992; Pereira et al., 2011) and are thought to settle within tens of kilometres maximum (Gaylord et al., 2002).

The sea-urchins' population status also critically shapes the patterns of abundance, distribution and functioning of kelp forests through grazing behaviour (Filbee-Dexter and Scheibling, 2014). Events of overgrazing can lead to severe reductions in plant biomass and in extreme cases to impoverished urchin barrens (Ling et al., 2015). The recovery of canopy-forming macroalgae assemblages in coastal areas of Madeira seems to have been inhibited by decades of sea-urchin barrens (Bernal-Ibáñez et al., 2021). However, the community of the Madeira-Desertas Ridge appears quite fit with few urchins of *A. lixula* (90–112 m) and without signs of moderate to intense grazing on kelps. Intense grazing on *Laminaria* has been documented off mainland Portugal, and has been recognised as the cause of the *Laminaria* population decay there (Franco et al., 2015). Yet, those authors found out that grazing intensity by sea urchins and herbivorous fish was lower at colder (open reefs) than at warmer regions, where this negative balance between production and consumption was driving kelp recruits "into hiding" in crevices. While net recruitment success might be compromised for macroalgae occurring in the coastal areas of Madeira Island, the deep ridge plateau likely provides a topographical refuge from grazing.

This apparent "stable state" could also result from the high abundance of sparid and labrid fishes (e.g., *C. julis*) inside the kelp forest that might be regulating the prey population. These fish prey upon sea urchins, including *A. lixula*, of several range sizes with sparids preferring small (<1 cm in test diameter) to medium (1–4 cm) urchins and labrids only prey upon small urchins (Guidetti, 2004). In the absence of predatory fishes (e.g., overfishing) grazer blooms may occur such as the one observed

during the 1970s that depleted more than 2000 km^2 of a *L. hyperborea* forest along Norwegian and Russian coasts (Norderhaug et al., 2021).

Ultimately, and likely the primary driver, regards to the hydrodynamic regime recorded nearby (and inside) the kelp forest that combines bidirectional wave-induced forces mixed with seabed currents, and local upwelling. Besides sea surface water currents on average faster than at surrounding areas, which might increase growth and productivity rates of macroalgae communities (Hurd, 2017), the ridge also experiences a pronounced wave action in its plateau. This is another main environmental variable shaping global distribution of kelp biome, where there is a low probability of kelp occurrence in the absence of waves (Jayathilake and Costello, 2020). While water motion can free blade surfaces from sedimentation, scour and epiphytic growth, light trapping area available for photosynthesis can be maximised improving nutrient uptake (e.g., nitrogen) across thinner diffusion boundary layers (Kregting et al., 2013; Hurd, 2017). On the other hand, the lower significant wave heights and lower wave periods herein recorded can inhibit dislodgement and breakage usually observed under high wave exposure (energy) scenarios or storms (Byrnes et al., 2011).

Adding to that, the presence of a cyclonic-like vortice structure at the study area (Figures 4) indicates local upwelling with colder and enriched nutrient waters supplied to surface (Lévy et al., 2018). In general, these vortices have pronounced impacts on biological processes, tracer transport, and properties of the water column, and can remain coherent for several months (Chelton et al., 2011; Zhang et al., 2014). For the kelps of the ridge that otherwise experience low nutrient levels (Longhurst, 1995; Narciso et al., 2019), such water flows are valuable resources for recruitment, growth, reproduction and stress tolerance (e.g., Graham et al., 2007). Likewise, the high concentrations of chlorophyll-α and dissolved oxygen reflect elevated phytoplankton densities or even blooms, with these primary producers largely profiting from those nutrient pulses to expand their biomass, which in turn causes a higher water light attenuation (also partly due to the elevated CDOM).

Field measurements strongly support these interpretations from the satellite imagery. First, the highest dissolved oxygen concentrations were both recorded at the nearest CTD station (WFS) of the kelp forest at depths between 10-70 m and inside this biotope (Table 2). Secondly, the DIN, phosphates, and silicates were low at the euphotic zone in contrast with elevated nutrient concentrations near seabed at the deepest station (~334 m), where an unusually high (25.50) Redfield's N:P ratio was found. These findings indicate nutrient depletion during phytoplankton biomass increase, and at the same time, nutrient supply to support kelp growth (Franco et al., 2018), including of nitrate and phosphate that are within the top three abiotic variables found to control *L. ochroleuca* distribution (Jayathilake and Costello, 2020). Taken together, results suggest high surface primary productivity at the top of the ridge that is highly favourable to overlying sessile megabenthic communities characterised by benthic suspension feeders (biotopes 1-4).

The biotope 4 represents the first monospecific coral garden of *P.* cf. *grayi* contrasting with descriptions of mixed gorgonian assemblages in other temperate coralligenous reef habitats (Altuna Prados, 1991). It also stands as an important habitat provider of enhanced biodiversity due to the high number of species observed that was within recorded values in the other biotopes occupying much wider areas (Thomsen et al., 2010).

The high densities observed for *P.* cf. *grayi* up to 0.3 colonies p/m^2 were three times more than the threshold used to classify a coral garden (Bullimore et al., 2013), which clearly reflects the conducive growth conditions of this mesophotic spot. Its diet varies from zooplankton to particulate organic matter (Coma et al., 1994; Ribes et al., 1999), and therefore food supply can be both enhanced by the local hydrodynamic regime (convective currents and waves) and pronounced phytoplankton productivity that boosts zooplankton biomass. Moreover, kelp forests can locally increase the saturation states of aragonite and calcite and by doing that encourage calcification processes in the surrounding environment (Murie and Bourdeau, 2020). Therefore, it is also possible that *P.* cf. *grayi* took advantage of its proximity with kelps by enhancing their sclerite production, which is used for skeleton support in gorgonians. The presence of many other calcifying organisms, such as calcareous algae, sponges and the scleractinian *Dendrophyllia ramea*, partly also due to the coralline-encrusted bedrock (Priede et al., 2013), agrees with those putative fine-scale changes in seawater chemistry. As such, it seems that the ridge offers not only potential for a deep refuge for kelps of ocean warming, but also for calcifiers of acidification stress.

But why was the *Paramuricea* biotope within a few meters' depth range? One possible driver often reported in sister species consists of short dispersal distances that can limit gene flow (Coma et al., 1995). However, this hypothesis is difficult to ascertain due to the lack of reproductive data. Another option relates to environmental gradients, such as properties (physical and chemical) and stratification of water mass layers. In the Gulf of Mexico, at least five *Paramuricea* species exhibited strong segregation by depth in response to distinct water mass layers (Doughty et al., 2014). In Canada, overlapping bathymetric distributions (150-1500 m) related to the homogenous Labrador Sea were reported (Radice et al., 2016). At the ridge, the *Paramuricea* biotope was exposed to the lower limit of the boundary between the MLD and the ENACW. Since the latter is colder, less dense, and more nutrient deprived, the control of *P.* cf. *grayi* distribution also appears to lie on the influence of water masses.

The biotope immediately below (3) represents the first description of a mesophotic black coral garden at soft bottoms in the NE Atlantic, on which *Antipathes* sp. was the dominant

species on level sandy bottom. Most of what we know on black coral habitats at depths beyond the range of recreational scuba diving in this ocean basin are built on descriptions of *Antipathella wollastoni* (Canary Islands) and *Antipathella subpinnata* (Azores and southwestern coast of mainland Portugal) in rocky substrates with these species forming bush-like colonies up to 0.7-1 m height (de Matos et al., 2014; Czechowska et al., 2020; Nestorowicz et al., 2021). *Antipathes* sp. is much more fragile creating smaller colonies up to 20cm in height, which may explain why this species occurred deeper at low (<10°) (substrate) slope with only a small part of its range extending throughout the mid slope. In that way, colonies are exposed to moderate current flows, and consequently, more protected from the hydrodynamic pressure on top of the ridge and stronger slope currents below (Bo et al., 2009; Wagner et al., 2012). The remarkable densities found across the mesophotic-aphotic depth gradient (ecotone) suggest preference for low-light environments, a trait shared by many antipatharians (Wagner et al., 2012). As a zooplankton predator, feeding rhythms and prey capture success can also be improved in highly productive areas, which may be the reason for such enhanced growth (Wagner et al., 2012).

Upper and deep slope

Two hard bottom coral gardens were observed at the deepest ("aphotic") environment with the gorgonians *E. verrucosa* (biotope 2, 173–252 m) and *V. flagellum* (biotope 1, 252–366 m) forming sparse to moderate assemblages, i.e., 3.1 and 4.8 colonies p/100m^2, respectively. The former biotope found at the upper slope differs from the typical mixed coral gardens found at continental shelf habitats of the NE Atlantic (~down to 200m depth) that are dominated by *Paramuricea* spp. and other branched gorgonians including *Eunicella* spp. (e.g., Nestorowicz et al., 2021). Although more sparsely distributed than other indicator gorgonian species from neighbouring biotopes, *E. verrucosa* together with *Antipathes* sp. and several sponge species (*P. monilifera*, cf. *Pseudotrachya hystrix* and Axinellidae Indet.) created herein conspicuous assemblages on both exposed bedrock and bedrock with a sediment cover that could be related to the higher substrate complexity and previously mentioned hydrodynamic conditions offered by the ridge.

Regarding biotope 1, results are aligned with the known habitat preferences of *V. flagellum* for steep (69–74°) slopes and seabed of low (0–0.2) rugosity (Giusti et al., 2017). This whip coral is known to create dense coral gardens (~120-450m depths) in its Eastern Atlantic-Mediterranean distribution, which can be monospecific (Ramos et al., 2016; Chimienti et al., 2021) or mixed with other gorgonian species such as *D.* aff. *meteor* or *P. hirsuta, Bebryce mollis* and *Villogorgia bebrycoides* in the Azores (Braga-Henriques, 2014) and *Callogorgia verticillata* and *E. verrucosa* in the Mediterranean Sea (Aguilar et al., 2006). To the best of our knowledge, only once colonies of *V. flagellum* and fan-shaped sponges of axinellid (cf. *Phakellia ventilabrum*) and Astrophorina-like species were reported clustering at the same depth strata (140-170m, Ormond peak), but those assemblages were not classed as mixed *V. flagellum* gardens (Ramos et al., 2016). Despite the presence of axinellids (including *Phakellia*) in the mixed *Viminella* and sponge garden biotope of the deep slope, Astrophorina sponges were substantially more abundant with *P. monilifera* reaching densities of 21 individuals p/100m^2. The assemblage structure so far unknown within hard bottom coral gardens dominated by *V. flagellum* (e.g., ICES, 2020) might be explained by species-specific morphological traits that are more advantageous to cope with stronger currents and enhanced sediment flows along steep slopes. While *Phakellia*-like spp. are structurally fragile exhibiting a thin peduncle for seabed attachment, *Pachastrella* species are more robust (compact) with a much wider body area attached to the substrate thus allowing for a higher stability on seabed. Likewise, *V. flagellum* exhibits a strong calcified axis that firmly attaches to the seabed and a flexible body with non-retractile polyps favourable to food particle capture in high energetic flows.

Implications for conservation

Our research identified a deep-water hotspot of biological diversity in Madeira that likely contributes to the provision of dispersal corridors of foundation species at the central NE Atlantic. Except for maërl, the newfound biotopes of conservation priority (EC Habitats Directive, the Marine Strategy Framework Directive, United Nations General Assembly and the OSPAR Convention) were previously not known to exist in this region demonstrating the Madeira-Desertas Ridge potential for a climate refugia hotspot for deep benthic communities dominated by kelp and long-lived calcifiers (corals, sponges). The kelp forest and temperate gorgonian (*Paramuricea*) garden at the mesophotic zone may also be considered Essential Fish Habitats (NMFS, 2002), in view of the high number of juvenile fish specimens observed. Furthermore, habitats with high densities of branched gorgonians (MAFs) cause significant changes in seabed substrate and flow conditions of the surrounding environment, with substantial gains in terms of necto-benthic biomass (Cerrano et al., 2010).

Such discoveries nearby the easternmost sector of the southern coastline of Madeira Island (~ 8Km) where various activities of coastal development occur, such as heavy ship traffic (commercial port of Caniçal) and offshore fish farming, encourage effective conservation measures in further spatial planning. These stressors are drivers of increased sedimentation rates, water turbidity and

pollution in the surrounding environment that may lead to biodiversity losses with subsequent impacts on ecosystem functioning (Sanz-Lázaro et al., 2011; Scherner et al., 2013; Girard and Fisher, 2018). Also of note is the observation of lost fishing lines and damaged gorgonians in the coral garden biotopes, indicating some level of fishing pressure on these communities. Cumulative fishing impacts could affect community functional diversity, and therefore, lead to ecosystem disruption (Yachi and Loreau, 1999; Buhl-Mortensen et al., 2022). Adding to that, global declines linked with ocean warming have been documented in many vhabitat-forming species including kelps that have distributional ranges climatically shaped, thus threatening their stability and persistence in the long-term (Smale, 2020). This is particularly true for *L. ochroleuca* that has a more limited physiological plasticity than other Lusitanian kelps, and therefore can be more vulnerable to a heating up ocean (Biskup et al., 2014). Taken together, results underscore the importance of taking critical actions to sustain these biodiversity hotspots across time. The great number of singular deep biotopes in such a relatively limited area is indeed remarkable, and consequently, challenging in terms of conservation and long-term investigations. Although this feature is lightly protected as a Site of Community Importance (SCI) for Cetaceans under the Natura 2000 network it meets so many other ecological criteria for a broader Marine Protected Area that new measures should be considered to include the protection of the mesophotic and deep-sea habitats.

Data availability statement

The data presented in the study are deposited in the GenBank repository, accession numbers ON951970, ON951971.

Author contributions

AB-H, PB-M, and MB: conceptualization. AB-H and PB-M: methodology. AB-H, PB-M, ET, AM, TS, KJ, JJ, TV, and MB: data acquisition and analyses. AB-H and PB-M: writing – original draft; AB-H writing – final draft; All authors edited and approved this manuscript.

Funding

This work was supported by the DEEP-ML project (MAR2020-P06M02-0535P) from the Regional Secretariat for the Environmental, Natural Resources and Climate Change (SRAAC) of the Regional Government of Madeira through the MAR 2020 operational programme under the European Maritime and Fisheries Fund, the Portuguese Foundation for Science and Technology (FCT) through the strategic project [UIDB/04292/2020] granted to MARE & project [LA/P/0069/2020] granted to the Associate Laboratory ARNET, iFADO project for postdoc grant to ET (M3.1aBGCT/F/001/BGCT/2018), ARDITI for PhD grant to TS (SFRH/BD/04292/2019), and Scientific Employment Stimulus FCT programme for CEEC individual contract to JC-C (CEECINST/00098/2018). AB-H was partly supported by the Oceanic Observatory of Madeira project (M1420-01-0145-FEDER-000001-Observatório Oceânico da Madeira-OOM) co-financed by the Madeira Regional Operational Programme (Madeira 14-20) under the Portugal 2020 strategy through the European Regional Development Fund https://ec.europa.eu/regional_policy/en/funding/erdf/2014-2020.

Acknowledgments

Many thanks are due to the Regional Government of Madeira (Manuel Ara Oliveira, Paula Menezes, Susana Prada, Nádia Coelho, Pedro Sepúlveda & team) and Focus Natura Dive Center (Pedro Vasconcelos). Dr. Kenneth Meland from the Marine Biodiversity Group, University of Bergen for genetic analysis. Dr. Manfred Kaufmann, PI of the MPhytoLab (University of Madeira) for equipment and reagents used in nutrient analysis. Crew of ADA REBIKOFF (Hugo Silva and Ana Jakobsen) from support in sea missions and dive operations. Captain, crew and scientific team (Ana Nóbrega, Elizabeth Akoulina) of "Monaco Explorations 2017–2020" for field and lab work that provided the position coordinates of a potential kelp habitat in Madeira.

Conflict of interest

The authors declare that the research was conducted in the absence of any commercial or financial relationships that could be construed as a potential conflict of interest.

Publisher's note

All claims expressed in this article are solely those of the authors and do not necessarily represent those of their affiliated organizations, or those of the publisher, the editors and the reviewers. Any product that may be evaluated in this article, or claim that may be made by its manufacturer, is not guaranteed or endorsed by the publisher.

Supplementary material

The Supplementary Material for this article can be found online at: https://www.frontiersin.org/articles/10.3389/fmars.2022.973364/full#supplementary-material

References

Aguilar, R., Pastor, X., and de Pablo, M. J. (2006). *Habitats in danger* (Oceana: Fundación Biodiversidad).

Altuna Prados, A. (1991). Nota sobre la presencia de *Paramuricea grayi* (Johnson, 1861) (Cnidaria, Anthozoa) en la costa vasca. *Munibe* 43, 85–90.

Amorim, P., Atchoi, E., and Tempera, F. (2015). Infralittoral mapping around an oceanic archipelago using MERIS FR satellite imagery and deep kelp observations: A new tool for assessing MPA coverage targets. *J. Sea Res.* 100, 120–132. doi: 10.1016/j.seares.2014.10.002

Assis, J., Serrão, E. A., Coelho, N. C., Tempera, F., Valero, M., and Alberto, F. (2018). Past climate changes and strong oceanographic barriers structured low-latitude genetic relics for the golden kelp *Laminaria ochroleuca*. *J. Biogeogr.* 45 (10), 2326–2336. doi: 10.1111/jbi.13425

Batten, M. L., Martinez, J. R., Bryan, D. W., and Buch, E. J. (2000). A modelling study of the coastal eastern boundary current system off Iberia and Morocco. *J. Geophysical Res.* 105, 14173–14195. doi: 10.1029/2000JC900026

Beaumont, N. J., Austen, M. C., Mangi, S. C., and Townsend, M. (2008). Economic valuation for the conservation of marine biodiversity. *Mar. Pollut. Bull.* 56, 386–396. doi: 10.1016/j.marpolbul.2007.11.013

Bekkby, T., Smit, C., Gundersen, H., Rinde, E., Steen, H., Tveiten, L., et al. (2019). The abundance of kelp is modified by the combined impact of depth, waves and currents. *Front. Mar. Sci.* 6, 475. doi: 10.3389/fmars.2019.00475

Bernal-Ibáñez, A., Cacabelos, E., Melo, R., and Gestoso, I. (2021). The role of sea-urchins in marine forests from Azores, Webbnesia, and Cabo Verde: human pressures, climate-change effects and restoration opportunities. *Front. Mar. Sci.* 8, 649873. doi: 10.3389/fmars.2021.649873

Birkett, D. A., Maggs, C. A., Dring, M. J., and Boaden, P. J. S. (1998). "Infralittoral reef biotopes with kelp species (volume VII)," in *An overview of dynamic and sensitivity characteristics for conservation management of marine SACs* (Oban: Scottish Association of Marine Science (UK Marine SACs Project), 174.

Biskup, S., Bertocci, I., Arenas, F., and Tuya, F. (2014). Functional responses of juvenile kelps, *Laminaria ochroleuca* and *Saccorhiza polyschides*, to increasing temperatures. *Aquat. Bot.* 113, 117–122. doi: 10.1016/j.aquabot.2013.10.003

Boavida, J., Paulo, D., Aurelle, D., Arnaud-Haond, S., Marschal, C., Reed, J., et al. (2016). A well-kept treasure at depth: precious red coral rediscovered in Atlantic deep coral gardens (SW Portugal) after 300 years. *PloS One* 11, e0147228. doi: 10.1371/journal.pone.014722

Bo, M., Bavestrello, G., Canese, S., Giusti, M., Salvati, E., Angiolillo, M., et al. (2009). Characteristics of a black coral meadow in the twilight zone of the central Mediterranean Sea. *Mar. Ecol. Progr. Ser.* 397, 53–61. doi: 10.3354/meps08185

Bo, M., Bertolino, M., Borghini, M., Castellano, M., Covazzi Harriague, A., and Camillo, Di (2011). Characteristics of the mesophotic megabenthic assemblages of the Vercelli seamount (North Tyrrhenian Sea). *PloS One* 6 (2), e16357. doi: 10.1371/journal.pone.0016357

Borcard, D., Legendre, P., and Drapeau, P. (1992). Partialling out the spatial component of ecological variation. *Ecology* 73, 1045–1055. doi: 10.2307/1940179

Braga-Henriques, A. (2014). *Cold-water coral communities in the Azores: diversity, habitat and conservation. Ph.D. thesis* (Portugal: University of the Azores). Available at: http://hdl.handle.net/10400.3/3615.

Braga-Henriques, A., Porteiro, F. M., Ribeiro, P. A., de Matos, V., Sampaio, I., Ocaña, O., et al. (2013). Diversity, distribution and spatial structure of the cold-water coral fauna of the Azores (NE Atlantic). *Biogeosciences* 10, 4009–4036. doi: 10.5194/bg-10-4009-2013

Buhl-Mortensen, P., Braga-Henriques, A., and Stevenson, A. (2022). Polyp loss and mass occurrence of sea urchins on bamboo corals in the deep sea: an indirect effect of fishing impact? *Ecology* 103 (2), e03564. doi: 10.1002/ecy.3564

Bullimore, R. D., Foster, N. L., and Howell, K. L. (2013). Coral-characterized benthic assemblages of the deep northeast Atlantic: defining "Coral Gardens" to support future habitat mapping. *ICES J. Mar. Sci.* 70, 511–522. doi: 10.1093/icesjms/fss195

Byrnes, J. E., Reed, D. C., Cardinale, B. J., Cavanaugh, K. C., Holbrook, S. J., and Schmitt, R. J. (2011). Climate-driven increases in storm frequency simplify kelp forest food webs. *Glob. Change Biol.* 17, 2513–2524. doi: 10.1111/j.1365-2486.2011.02409.x

Cairns, S. D., and Bayer, F. M. (1908). Studies on Western Atlantic Octocorallia (Coelenterata: Anthozoa). Part 4: The genus *Paracalyptrophora* Kinoshita,. *Proc. Biol. Soc Wash.* 117 (1), 114–139.

Campuzano, F., Nunes, S., Malhadas, M., and Neves, R. (2010). Modelling the hydrodynamics and water quality of Madeira island (Portugal). *Globec Int. Newslett.* 16, 40–42.

Cerrano, C., Bastari, A., Calcinai, B., Di Camillo, C., Pica, D., Puce, S., et al. (2019). Temperate mesophotic ecosystems: gaps and perspectives of an emerging conservation challenge for the Mediterranean Sea. *Eur. Zool. J.* 86 (1), 370–388. doi: 10.1080/24750263.2019.1677790

Cerrano, C., Danovaro, R., Gambi, C., Pusceddu, A., Riva, A., and Schiaparelli, S. (2010). Gold coral (*Savalia savaglia*) and gorgonian forests enhance benthic biodiversity and ecosystem functioning in the mesophotic zone. *Biodivers. Conserv.* 19, 153–167. doi: 10.1007/s10531-009-9712-5

Chelton, D. B., Gaube, P., Schlax, M. G., Early, J. J., and Samelson, R. M. (2011). The influence of nonlinear mesoscale eddies on near-surface oceanic chlorophyll. *Science* 334 (6054), 328–332. doi: 10.1126/science.1208897

Chimienti, G., Aguilar, R., Maiorca, M., and Mastrototaro, F. A. (2021). Newly discovered forest of the whip coral *Viminella flagellum* (Anthozoa, Alcyonacea) in the Mediterranean Sea: A non-invasive method to assess its population structure. *Biology* 11 (1), 39. doi: 10.3390/biology11010039

Chung, I. K., Beardall, J., Mehta, S., Sahoo, D., and Stojkovic, S. (2011). Using marine macroalgae for carbon sequestration: a critical appraisal. *J. Appl. Phycol.* 23, 877–886. doi: 10.1007/s10811-010-9604-9

Clarke, G. L. (1936). Light penetration in the western North Atlantic and its application to biological problems. *Conseil Perm. Intern. p. l' Explor. la Mer, et Rapp. Proc.-Verb.* 101 (3), 1–14. doi: 10.17895/ices.pub.9190

CNEXO (1972). *Bathyscaphe "Archimède". Campagne 1966 à Madère, Campagne 1969 aux Açores. Publications du Centre National pour l'Exploitation des Océans (CNEXO), Série Résultats des Campagnes à la Mer*, Vol. 3. 1972, ISSN 0339-2902.

Colwell, R. K., and Lees, D. C. (2000). The mid-domain effect: Geometric constraints on the geography of species richness. *TREE* 15, 70–76. doi: 10.1016/S0169-5347(99)01767-X

Coma, R., Gili, J. M., Zabala, M., and Riera, T. (1994). Feeding and prey capture in the aposymbiontic gorgonian *Paramuricea clavata*. *Mar. Ecol. Prog. Ser.* 115, 257–270. doi: 10.3354/meps115257

Coma, R., Ribes, M., Zabala, M., and Gili, J. M. (1995). Reproduction and cycle of gonadal development in the Mediterranean gorgonian *Paramuricea clavata*. *Mar. Ecol. Prog. Ser.* 117, 173–183. doi: 10.3354/meps117173

Czechowska, K., Feldens, P., Tuya, F., Cosme de Esteban, M., Espino, F., Haroun, R., et al. (2020). Testing side-scan sonar and multibeam echosounder to study black coral gardens: a case study from macaronesia. *Remote Sens.* 12 (19), 3244. doi: 10.3390/rs12193244

de Matos, V., Gomes-Pereira, J. N., Tempera, F., Ribeiro, P. A., Braga-Henriques, A., and Porteiro, F. M. (2014). First record of *Antipathella subpinnata* (Anthozoa, antipatharia) in the Azores (NE Atlantic), with description of the first monotypic garden for this species. *Deep Sea Res. Part II Top. Stud. Oceanogr.* 99, 113–121. doi: 10.1016/j.dsr2.2013.07.003

Doughty, C. L., Quattrini, A. M., and Cordes, E. E. (2014). Insights into the population dynamics of the deep-sea coral genus *Paramuricea* in the gulf of Mexico. *Deep Sea Res. Part II Top. Stud. Oceanogr.* 99, 71–82. doi: 10.1016/j.dsr2.2013.05.023

Drew, E. A. (1974). An ecological study of *Laminaria ochroleuca* PYL. growing below 50 metres in the straits of Messina. *J. Exp. Mar. Biol. Ecol.* 15, 11–24. doi: 10.1016/0022-0981(74)90059-8

FAO (Food Agriculture Organization of the United Nations) (2009) *International Guidelines for the Management of Deep-Sea Fisheries in the High-Seas*. Available at: http://www.fao.org/fishery/topic/166308/en.

Figueiredo, M. A. O., Kain, J. M., and Norton, T. A. (2000). Responses of crustose corallines to epiphyte and canopy cover. *J. Phycol.* 36, 17–24. doi: 10.1046/j.1529-8817.2000.98208.x

Filbee-Dexter, K., and Scheibling, R. E. (2014). Sea urchin barrens as alternative stable states of collapsed kelp ecosystems. *Mar. Ecol. Prog. Ser.* 495, 1–25. doi: 10.3354/meps10573

Foster, M. S. (2001). Rhodoliths: between rocks and soft places. *J. Phycol.* 37, 659–667. doi: 10.1046/j.1529-8817.2001.00195.x

Franco, J. N., Tuya, F., Bertocci, I., Rodríguez, L., Martínez, B., Sousa-Pinto, I., et al. (2018). The 'golden kelp' *Laminaria ochroleuca* under global change: integrating multiple eco-physiological responses with species distribution models. *J. Ecol.* 106 (1), 47–58. doi: 10.1111/1365-2745.12810

Franco, J. N., Wernberg, T., Bertocci, I., Duarte, P., Jacinto, D., Vasco-Rodrigues, N., et al. (2015). Herbivory drives kelp recruits into 'hiding' in a warm ocean climate. *Mar. Ecol. Prog. Ser.* 536, 1–9. doi: 10.3354/meps11445

Gattuso, J.-P., Gentili, B., Duarte, C. M., Kleypas, J. A., Middelburg, J. J., and Antoine, D. (2006). Light availability in the coastal ocean: impact on the distribution of benthic photosynthetic organisms and their contribution to primary production. *Biogeosciences* 3, 489–513. doi: 10.5194/bg-3-489-2006

Gaylord, B., Nickols, K. J., and Jurgens, L. (2012). Roles of transport and mixing processes in kelp forest ecology. *J. Exp. Biol.* 215, 997–1007. doi: 10.1242/jeb.059824

Gaylord, B., Reed, D. C., Raimondi, P. T., Washburn, L., and McLean, S. R. (2002). A physically based model of macroalgal spore dispersal in the wave and current-dominated nearshore. *Ecology* 83, 1239–1251. doi: 10.1890/0012-9658(2002)083[1239:APBMOM]2.0.CO;2

Geldmacher, J., Hoernle, K., Klügel, A., van den Bogaard, P., and Duggen, S. (2006). A geochemical transect across a heterogeneous mantle upwelling: implications for the evolution of the Madeira hotspot in space and time. *Lithos* 90, 131–144. doi: 10.1016/j.lithos.2006.02.004

Girard, F., and Fisher, C. R. (2018). Long-term impact of the Deepwater Horizon oil spill on deep-sea corals detected after seven years of monitoring. *Biol. Conserv.* 225, 117–127. doi: 10.1016/j.biocon.2018.06.028

Giusti, M., Bo, M., Angiolillo, M., Cannas, R., Cau, A., Follesa, M. C., et al. (2017). Habitat preference of *Viminella flagellum* (Alcyonacea: Ellisellidae) in relation to bathymetric variables in southeastern Sardinian waters. *Cont. Shelf. Res.* 138, 41–50. doi: 10.1016/j.csr.2017.03.004

Gove, J. M., McManus, M. A., Neuheimer, A. B., Polovina, J. J., Drazen, J. C., Smith, C. R., et al. (2016). Near-island biological hotspots in barren ocean basins. *Nat. Commun.* 7, 10581. doi: 10.1038/ncomms10581

Graham, M. H., Kinlan, B. P., Druehl, L. D., Garske, L. E., and Banks, S. (2007). Deep-water kelp refugia as potential hotspots of tropical marine diversity and productivity. *Proc. Natl. Acad. Sci. U.S.A.* 104, 16576–16580. doi: 10.1073/pnas.0704778104

Grasshoff, M. (1992). Die Fachwasser-Gorgonarien von Europa und Westafrika (Cnidaria, Anthozoa). *Courier Forschungsinstitut Senckenberg* 149, 1–135.

Grasshoff, K., Kremling, K., and Ehrhardt, M. (1999). *Methods of seawater analysis* (Weinheim: WILEY-VCH). doi: 10.1002/9783527613984

Guidetti, P. (2004). Consumers of sea urchins, *Paracentrotus lividus* and *Arbacia lixula*, in shallow Mediterranean rocky reefs. *Helgol. Mar. Res.* 58, 110–116. doi: 10.1007/s10152-004-0176-4

Hill, M. O. (1973). Reciprocal averaging: An eigenvector method of ordination. *J. Ecol.* 61, 237–349. doi: 10.2307/2258931

Hill, M. O. (1979). *TWINSPAN a Fortran Program for Arranging Multivariate Data in an Ordered Two-Way Table by Classification of the Individuals and Attributes. Ecology and Systematic* (Ithaca, NY: Cornell University).

Hill, M. O., and Gauch, H. G. (1980). Detrended correspondence analysis: An improved ordination technique. *Vegetatio* 42, 47–58. doi: 10.1007/BF00048870

Howell, K. L., Davies, J. S., Allcock, A. L., Braga-Henriques, A., Buhl-Mortensen, P., Carreiro-Silva, M., et al. (2019). A framework for the development of a global standardised marine taxon reference image database (SMarTaR-ID) to support image-based analyses. *PloS One* 14 (12), e0218904. doi: 10.1371/journal.pone.0218904

Hurd, C. L. (2017). Shaken and stirred: The fundamental role of water motion in resource acquisition and seaweed productivity. *Perspect. Phycology* 4 (2), 73–81. doi: 10.1127/pip/2017/0072

ICES (2020). ICES/NAFO joint working group on deep-water ecology (WGDEC). *ICES Sci. Rep.* 2, 62. doi: 10.17895/ices.pub.7503

Jayathilake, D. R., and Costello, M. J. (2020). A modelled global distribution of the kelp biome. *Biol. Conserv.* 252, 108815. doi: 10.1016/j.biocon.2020.108815

John, D. M. (1969). An ecological study on *Laminaria ochroleuca*. *J. Mar. Biol. Ass. U.K.* 49, 175. doi: 10.1017/S0025315400046506

Johnson, J. Y. (1861). Description of a second species of *Acanthogorgia* (JE Gray) from Madeira. *Proc. Zool Soc. London* 1861, 296–298.

Kain, J. M. (1971). The biology of *Laminaria hyperborea*. VI. Some Norwegian populations. *J. Mar. Biol. Ass. U.K.* 51, 387–408. doi: 10.1017/S0025315400031866

Klein, B., and Siedler, G. (1989). *On the origin of the Azores Current. J. Geophysical Res.* 94, 6159–6168. doi: 10.1029/JC094iC05p06159

Klügel, A., Walter, T. R., Schwarz, S., and Geldmacher, J. (2005). Gravitational spreading causes en-echelon diking along a rift zone of Madeira archipelago: an experimental approach and implications for magma transport. *Bull. Volcanol.* 68, 37. doi: 10.1007/s00445-005-0418-6

Kregting, L. T., Blight, A. B., Elsäßer, B., and Savidge, G. (2013). The influence of water motion on the growth rate of the kelp *Laminaria hyperborea*. *J. Exp. Mar. Biol. Ecol.* 448, 337–345. doi: 10.1016/j.jembe.2013.07.017

Laverick, J. H., Andradi-Brown, D. A., and Rogers, A. D. (2017). Using light-dependent Scleractinia to define the upper boundary of mesophotic coral ecosystems on the reefs of Utila, Honduras. *PloS One* 12 (8), e0183075. doi: 10.1371/journal.pone.0183075

Lesser, M. P., Slattery, M., Laverick, J. H., Macartney, K. J., and Bridge, T. C. (2019). Global community breaks at 60 m on mesophotic coral reefs. *Global Ecol. Biog.* 28 (10), 1403–1416. doi: 10.1111/geb.12940

Lesser, M. P., Slattery, M., and Leichter, J. J. (2009). Ecology of mesophotic coral reefs. *J. Exp. Mar. Biol. Ecol.* 375, 1–8. doi: 10.1016/j.jembe.2009.05.009

Lester, S. E., Ruttenberg, B. I., Gaines, S. D., and Kinlan, B. P. (2007). The relationship between dispersal ability and geographic range size. *Ecol. Lett.* 10, 745–758. doi: 10.1111/j.1461-0248.2007.01070.x

Le Traon, P. Y., and De Mey, P. (1994). The eddy field associated with the Azores Front east of the Mid-Atlantic Ridge as observed by the GEOSAT altimeter. *J. Geophys. Res.* 99, 9907–9923. doi: 10.1029/93JC03513

Levin, L. A., and Dayton, P. K. (2009). Ecological theory and continental margins: Where shallow meets deep. *Trends Ecol. Evol.* 24, 606–617. doi: 10.1016/j.tree.2009.04.012

Lévy, M., Franks, P. J. S., and Smith, K. S. (2018). The role of submesoscale currents in structuring marine ecosystems. *Nat. Commun.* 9 (1), 4758. doi: 10.1038/s41467-018-07059-3

Ling, S. D., Scheibling, R. E., Johnson, C. R., Rassweiler, A., Shears, N., Connell, S. D., et al. (2015). Global regime-shift dynamics of catastrophic sea urchin overgrazing. *Philos. Trans. R. Soc Lond. B* 370, 20130269. doi: 10.1098/rstb.2013.0269

Liu, M., and Tanhua, T. (2021). Water masses in the Atlantic Ccean: characteristics and distributions. *Ocean Sci.* 17, 463–486. doi: 10.5194/os-17-463-2021

Longhurst, A. (1995). Seasonal cycles of pelagic production and consumption. *Prog. Oceanogr.* 36, 77–167. doi: 10.1016/0079-6611(95)00015-1

Loya, Y., Puglise, K. A., and Bridge, T. C. L. (2019). *Mesophotic Coral Ecosystems* (New York: Springer), 1003. doi: 10.1007/978-3-319-92735-0

Markager, S., and Sand-Jensen, K. (1992). Light requirements and depth zonation of marine macroalgae. *Mar. Ecol. Prog. Ser.* 88, 83–92. doi: 10.3354/meps088083

McCune, B., and Mefford, M. J. (2006). *PC-ORD: Multivariate Analysis of Ecological Data. MJM Software, Gleneden Beach, Oregon. Computer Software.*

Mittelstaedt, E. (1991). The ocean boundary along the northwest African coast: Circulation and oceanographic properties at the sea surface. *Prog. Oceanogr.* 26, 307–355. doi: 10.1016/0079-6611(91)90011-A

Murie, K. A., and Bourdeau, P. E. (2020). Fragmented kelp forest canopies retain their ability to alter local seawater chemistry. *Sci. Rep.* 10, 11939. doi: 10.1038/s41598-020-68841-2

Muth, A. F. (2012). Effects of zoospore aggregation and substrate rugosity on kelp recruitment success. *J. Phycol.* 48, 1374–1379. doi: 10.1111/j.1529-8817.2012.01211.x

Narciso, A., Caldeira, R., Reis, J., Hoppenrath, M., Cachão, M., and Kaufmann, M. (2019). The effect of a transient frontal zone on the spatial distribution of extant coccolithophores around the Madeira archipelago (Northeast Atlantic). *Estuar. Coast. Shelf Sci.* 223, 25–38. doi: 10.1016/j.ecss.2019.04.014

Nestorowicz, I.-M., Oliveira, F., Monteiro, P., Bentes, L., Henriques, N. S., Aguilar, R., et al. (2021). Identifying habitats of conservation priority in the São Vicente Submarine Canyon in southwestern Portugal. *Front. Mar. Sci.* 8, 672850. doi: 10.3389/fmars.2021.672850

Neves, P., Silva, J., Peña, V., and Ribeiro, C. (2021). "Pink round stones"–rhodolith beds: an overlooked habitat in Madeira archipelago. *Biodivers. Conserv.* 30, 3359–3383. doi: 10.1007/s10531-021-02251-2

New, A. L., Jia, Y., Coulibaly, M., and Dengg, J. (2001). On the role of the Azores Current in the ventilation of the North Atlantic ocean. *Prog. Oceanogr.* 48, 163–194. doi: 10.1016/S0079-6611(01)00004-0

NMFS (National Marine Fisheries Service) (2002). Magnuson-Stevens Act Provisions, Essential Fish Habitat (EFH), Final rule. *Federal Register* 67 (12), 2343–2383.

Norderhaug, K. M., Nedreaas, K., Huserbråten, M., and Moland, E. (2021). Depletion of coastal predatory fish sub-stocks coincided with the largest sea urchin grazing event observed in the NE Atlantic. *Ambio* 50, 163–173. doi: 10.1007/s13280-020-01362-4.

Otero-Ferrer, F., Cosme, M., Tuya, F., Espino, F., and Haroun, R. (2020). Effect of depth and seasonality on the functioning of rhodolith seabeds. *Est. Coast. Shelf Sci.* 235, 106579. doi: 10.1016/j.ecss.2019.106579

Otto, L., and van Aken, H. M. (1996). Surface circulation in the northeast Atlantic as observed with drifters. *Deep Sea Res. Part I: Oceanogr. Res. Pap.* 43, 467–499. doi: 10.1016/0967-0637(96)00017-9

Pelegrí, J. L., and Peña-Izquierdo, J. (2015). "Eastern boundary currents off North-West Africa," *In: Oceanographic and biological features in the Canary Current Large Marine Ecosystem*, vol. 115 . Eds. L. Valdés and I. Déniz-González (Paris: IOC- UNESCO), 81–92. Available at: http://hdl.handle.net/1834/9179. IOC Technical Series, No. 115

Peña, V., Bárbara, I., Grall, J., Maggs, C. A., and Hall-Spencer, J. M. (2014). The diversity of seaweeds on maërl in the NE Atlantic. *Mar. Biodivers.* 44 (4), 533–551. doi: 10.1007/s12526-014-0214-7

Pereira, T. R., Engelen, A. H., Pearson, G., Serrão, E., Destombe, C., and Valero, M. (2011). Temperature effects on gametophyte development of *L. ochroleuca* and *S. polyschides*, kelps with contrasting life histories. *Cahiers Biologie Mar.* 52 (5), 395–403. doi: 10.21411/CBM.A.EE62BC68

Pessarrodona, A., Moore, P. J., Sayer, M. D. J., and Smale, D. A. (2018). Carbon assimilation and transfer through kelp forests in the NE Atlantic is diminished under a warmer ocean climate. *Glob. Change Biol.* 24, 4386–4398. doi: 10.1111/gcb.14303

Pica, D., Calcinai, B., Poliseno, A., Trainito, E., and Cerrano, C. (2018). Distribution and phenotypic variability of the Mediterranean gorgonian *Paramuricea macrospina* (Cnidaria: Octocorallia). *Eur. Zoological J.* 85 (1), 392–408. doi: 10.1080/24750263.2018.1529202

Ponti, M., Turicchia, E., Ferro, F., Cerrano, C., and Abbiati, M. (2018). The understorey of gorgonian forests in mesophotic temperate reefs. *Aquat. Conserv.: Mar. Freshw. Ecosyst.* 28, 1153–1166. doi: 10.1002/aqc.2928

Priede, I. G., Bergstad, O. A., Miller, P. I., Vecchione, M., Gebruk, A., Falkenhaug, T., et al. (2013). Does presence of a mid-ocean ridge enhance biomass and biodiversity? *PloS One* 8 (5), e61550. doi: 10.1371/journal.pone.0061550

Quartau, R., Ramalho, R. S., Madeira, J., Santos, R., Rodriques, A., Roque, C., et al. (2018). Gravitational, erosional and depositional processes on volcanic ocean islands: insights from the submarine morphology of Madeira archipelago. *Earth Planet. Sci. Lett.* 482, 28–299. doi: 10.1016/j.epsl.2017.11.003

Radice, V. Z., Quattrini, A. M., Wareham, V. E., Edinger, E. N., and Cordes, E. E. (2016). Vertical water mass structure in the North Atlantic influences the bathymetric distribution of species in the deep-sea coral genus *Paramuricea*. *Deep Sea Res. Part II: Top. Stud. Oceanogr.* 116, 253–263. doi: 10.1016/j.dsr.2016.08.014

Ramos, M., Bertocci, I., Tempera, F., Calado, G., Albuquerque, M., and Duarte, P. (2016). Patterns in megabenthic assemblages on a seamount summit (Ormonde Peak, Gorringe Bank, Northeast Atlantic). *Mar. Ecol.* 37, 1057–1072. doi: 10.1111/maec.12353

Redfield, A. C. (1934). On the proportions of organic derivatives in sea water and their relation to the composition of plankton, in James Johnstone memorial volume. (Liverpool, UK: Univ. Liverpool) pp, 176–192.

Reed, D. C., Amsler, C. D., and Ebeling, A. W. (1992). Dispersal in kelps: Factors affecting spore swimming and competency. *Ecology* 73, 1577–1585. doi: 10.2307/1940011

Reed, J. K., and Pomponi, S. A. (1992). "Eastern Atlantic Expedition: Submersible and scuba collections for bioactive organisms from the Azores to western Africa. International Pacifica Scientific Diving…1991," in *Proceedings of the American Academy of Underwater Sciences, 11th Annual Scientific Diving Symposium, Honolulu, Hawaii, American Academy of Underwater Sciences*, 65–74.

Ribes, M., Coma, R., and Gili, J. M. (1999). Heterogeneous feeding in benthic suspension feeders: the natural diet and grazing rate of the temperate gorgonian *Paramuricea clavata* (Cnidaria: Octocorallia) over a year cycle. *Mar. Ecol. Prog. Ser.* 183, 125–137. doi: 10.3354/meps183125

Rossi, S., Bramanti, L., Gori, A., and Orejas, C. (2017). "An overview of the animal forests of the world", in *Marine Animal Forests - The Ecology of Benthic Biodiversity Hotspots*. Eds. S. Rossi, L. Bramanti, A. Gori and C. Orejas (Springer Cham), 1–26. doi: 10.1007/978-3-319-17001-5_1-1

Ryther, J. H. (1956). Photosynthesis in the ocean as a function of light intensity. *Limnol. Oceanogr.* 1 (1), 61–70. doi: 10.4319/lo.1956.1.1.0061

Sanz-Lázaro, C., Belando, M. D., Lázaro Marín-Guirao, L., Navarrete-Mier, F., and Arnaldo, M. A. (2011). Relationship between sedimentation rates and benthic impact on Maërl beds derived from fish farming in the Mediterranean. *Mar. Environ. Res.* 71, 22–30. doi: 10.1016/j.marenvres.2010.09.005

Schäfer, S., Monteiro, J., Castro, N., Rilov, G., and Canning-Clode, J. (2019). *Cronius ruber* (Lamarck, 1818) arrives to Madeira island: a new indication of the ongoing tropicalization of the northeastern Atlantic. *Mar. Biodivers.* 49, 2699–2707. doi: 10.1007/s12526-019-00999-z

Scherner, F., Horta, P. A., de Oliveira, E. C., Simonassi, J. C., Hall-Spencer, J. M., Chow, F., et al. (2013). Coastal urbanization leads to remarkable seaweed species loss and community shifts along the SW Atlantic. *Mar. Pollut. Bull.* 76, 106–115. doi: 10.1016/j.marpolbul.2013.09.019

Schubert, N., Peña, V., Salazar, V. W., Horta, P. A., Neves, P., and Ribeiro, C. (2022). Rhodolith physiology across the Atlantic: towards a better mechanistic understanding of intra- and interspecific differences. *Front. Mar. Sci.* 9, 921639. doi: 10.3389/fmars.2022.921639

Silva, F. A., and Menezes, C. A. (1940). *Elucidário Madeirense (2nd edition, largely updated)*, Vol. I, A-E. 431. Junta Geral do Distrito Autónomo do Funchal. pp.+VII, Funchal (in pt.).

Smale, D. A. (2020). Impacts of ocean warming on kelp forest ecosystems. *New Phytol.* 225, 1447–1454. doi: 10.1111/nph.16107

Smale, D. A., and Wernberg, T. (2009). Satellite-derived SST data as a proxy for water temperature in nearshore benthic ecology. *Mar. Ecol. Prog. Ser.* 387, 27–37. doi: 10.3354/meps08132

Stefanoudis, P. V., Rivers, M., Smith, S. R., Schneider, C. W., Wagner, D., Ford, H., et al. (2019). Low connectivity between shallow, mesophotic and rariphotic zone benthos. *R. Soc. Open Sci.* 6, 190958. doi: 10.1098/rsos.190958

Teagle, H., Moore, P. J., Jenkins, H., and Smale, D. A. (2018). Spatial variability in the diversity and structure of faunal assemblages associated with kelp holdfasts (*Laminaria hyperborea*) in the northeast Atlantic. *PloS One* 13, e0200411. doi: 10.1371/journal.pone.0200411

Teira, E., Mourino, B., Maranon, E., Perez, V., Pazo, M. J., and Serret, P. (2005). Variability of chlorophyll and primary production in the Eastern North Atlantic subtropical gyre: Potential factors affecting phytoplankton activity. *Deep Sea Res. Part I: Oceanogr. Res. Pap.* 52, 569–588. doi: 10.1016/j.dsr.2004.11.007

Thomsen, M. S., Wernberg, T., Altieri, A., Tuya, F., Gulbransen, D., McGlathery, K. J., et al. (2010). Habitat cascades: the conceptual context and global relevance of facilitation cascades *via* habitat formation and modification. *Integr. Comp. Biol.* 50, 158–175. doi: 10.1093/icb/icq042

tom Dieck (Bartsch), I. (1992). North Pacific and North Atlantic digitate *Laminaria* species (Phaeophyta): hybridization experiments and temperature responses. *Phycologia* 31, 147–163. doi: 10.2216/i0031-8884-31-2-147.1

Tuya, F., Cacabelos, E., Duarte, P., Jacinto, D., Castro, J. J., Silva, T., et al. (2012). Patterns of landscape and assemblage structure along a latitudinal gradient in ocean climate. *Mar. Ecol. Prog. Ser.* 466, 9–19. doi: 10.3354/meps09941

Tuya, F., Fernández-Torquemada, Y., del Pilar-Ruso, Y., Espino, F., Manent, P., Curbelo, L., et al. (2021). Partitioning resilience of a marine foundation species into resistance and recovery trajectories. *Oecologia* 196, 515–527. doi: 10.1007/s00442-021-04945-4

van den Hoek, C. (1982). The distribution of benthic marine algae in relation to the temperature regulation of their life histories. *Biol. J. Linn. Soc.* 18 (2), 81–144. doi: 10.1111/j.1095-8312.1982.tb02035.x

Wagner, D., Luck, D. G., and Toonen, R. J. (2012). The biology and ecology of black corals (Cnidaria: Anthozoa: Hexacorallia: Antipatharia). *Adv. Mar. Biol.* 63, 67–132. doi: 10.1016/B978-0-12-394282-1.00002-8

Wentworth, C. K. (1922). A scale of grade and class terms for clastic sediments. *J. Geol.* 30, 377–392. doi: 10.1086/622910

Wernberg, T., Krumhansl, K., Filbee-Dexter, K., and Pedersen, M. F. (2019). "Status and trends for the world's kelp forests," in *World seas: An environmental evaluation*, *2nd* Academic Press, vol. III. Ed. C. Sheppard, 57–78. doi: 10.1016/B978-0-12-805052-1.00003-6

Yachi, S., and Loreau, M. (1999). Biodiversity and ecosystem productivity in a fluctuating environment: the insurance hypothesis. *Proc. Natl. Acad. Sci. U.S.A.* 96, 1463–1468. doi: 10.1073/pnas.96.4.1463

Yesson, C., Bush, L. E., Davies, A. J., Maggs, C. A., and Brodie, J. (2015). The distribution and environmental requirements of large brown seaweeds in the British isles. *J. Mar. Biol. Assoc. UK* 95, 669–680. doi: 10.1017/S0025315414001453

Zhang, Z., Wang, W., and Qiu, B. (2014). Oceanic mass transport by mesoscale eddies. *Science* 345 (6194), 322–324. doi: 10.1126/science.1252418